

Effective potential and first-order phase transitions: Beyond leading order

Peter Arnold

Department of Physics, University of Washington, Seattle, Washington 98195

Olivier Espinosa

Department of Physics, University of Washington, Seattle, Washington 98195

*Departamento de Física, Universidad Técnica, Federico Santa María, Casilla 110-V, Valparaíso, Chile**

(Received 11 December 1992)

Scenarios for electroweak baryogenesis require an understanding of the effective potential at finite temperature near a first-order electroweak phase transition. Working in the Landau gauge, we present a calculation of the dominant two-loop corrections to the ring-improved one-loop potential in the formal limit $g^4 \ll \lambda \ll g^2$, where λ is the Higgs self-coupling and g is the electroweak coupling. The limit $\lambda \ll g^2$ ensures that the phase transition is significantly first order, and the limit $g^4 \ll \lambda$ allows us to use high-temperature expansions. We find corrections from 20% to 40% at Higgs-boson masses relevant to the bound computed for baryogenesis in the minimal standard model. Though our numerical results seem to still rule out minimal standard model baryogenesis, this conclusion is not airtight because the loop expansion is only marginal when corrections are as big as 40%. We also discuss why superdaisy approximations do not correctly compute these corrections.

PACS number(s): 11.15.Kc, 05.70.Fh, 12.15.Cc, 98.80.Cq

I. INTRODUCTION

Recent scenarios [1–5] for baryogenesis via the baryon-number anomaly of the standard model have stimulated a flurry of investigation into the details of the electroweak phase transition in the hot, early Universe. Sakharov's generic conditions for baryogenesis [6] require (1) baryon-number violation, (2) CP violation, and (3) disequilibrium. In recent scenarios, the source of baryon number violation is a standard model effect, arising because baryon number has an electroweak anomaly and so is violated by nonperturbative physics. The rate of such violation is of order $\exp[-E_{\text{sp}}(T)/T]$ where T is the temperature, $E_{\text{sp}}(T) \sim \pi\sigma(T)/g_w$ is the electroweak sphaleron mass, and $\sigma(T)$ is the Higgs vacuum expectation value (VEV) at high temperature [7–10]. In almost all scenarios, disequilibrium is provided by bubble nucleation and expansion during a first-order electroweak phase transition. The requirement that the first-order phase transition be sufficiently strong then places constraints on models of the Higgs sector. In particular, it is necessary that baryon-number violation be turned off after the phase transition is completed; otherwise, the Universe will simply relax back to equilibrium, where the net baryon number is zero. Since the rate of baryon-number violation is exponentially sensitive to the VEV $\sigma(T)$, it is important to study the minimum $\phi = \sigma(T)$ of the finite-temperature effective potential $V(\phi, T)$ just after the phase transition. The purpose of this paper is to study the extent to which two-loop effects modify the re-

sults that have been found using one-loop approximations to the effective potential.

In this paper, for the sake of simplicity, we shall focus on the minimal standard model with a single Higgs doublet. Many of our calculations should be easily extendable to more complicated Higgs sectors. Most scenarios for electroweak baryogenesis are based on multi-Higgs models because the CP violation required for baryogenesis can be incorporated by CP -violating interactions in the Higgs sector, where it directly affects classical processes involving the sphaleron. It has been suggested, however, that the standard CP violation of the quark sector may by itself provide sufficient CP violation, so that even the minimal standard model, with a single Higgs doublet, could be viable [11]. In the minimal standard model, and using the one-loop ring-improved effective potential (which we review later), Dine *et al.* [12] have established an upper bound of roughly 30–40 GeV on the Higgs-boson mass $m_H(0)$ (measured at zero temperature) if baryogenesis is to occur at the weak phase transition. This scenario is then excluded by the experimental bound of $m_H(0) > 60$ GeV [13]. (These particular constraints may be evaded by models with more than one Higgs boson.)

An important question for such limits is whether they are significantly modified by higher-order corrections. As we shall review in the next section, the loop expansion parameter in this context turns out to be formally of order λ/g^2 , or equivalently $m_H(0)/M_W(0)$, where λ is the Higgs self-coupling and g is the $SU(2)$ gauge coupling. For the upper bound of Dine *et al.* on $m_H(0)$ of 30–40 GeV, it is not *a priori* clear whether $m_H(0)/M_W(0)$ is small—it all depends on the exact numerical coefficients in the loop expansion. Indeed, some of the earliest stud-

*Permanent address.

ies of corrections to the one-loop potential found large corrections, but these studies were subsequently shown to be flawed [12]. To resolve whether the bounds are reliable, we present an explicit computation of the dominant two-loop corrections to the one-loop ring-improved effective potential. Our objective is to compute the dominant corrections as the Higgs-boson mass gets large, but not so large that the loop expansion breaks down. Specifically, we assume

$$g^4 \ll \lambda \ll g^2. \quad (1.1)$$

(As we shall review in the next section, the lower limit $g^4 \ll \lambda$ simplifies the calculation by justifying a high-temperature expansion.) From the numerical results of this calculation, we shall determine the significance of multiloop corrections as a function of Higgs-boson mass; when we find numerical corrections of order 100% or more for a given Higgs-boson mass, we shall know that the loop expansion has indeed broken down.

The computation of such corrections has been previously attempted in the literature using a superdaisy approximation [14]. Unfortunately, as we discuss in Appendix C, the superdaisy approximation does not correctly compute the dominant corrections to the ring-improved one-loop potential.

Naively, we expect that corrections to the baryogenesis bounds should be small because the sphaleron is a classical solution of the effective high-temperature theory. The actions of classical solutions [in this case corresponding to the Boltzmann exponent $E_{\text{sp}}(T)/T$ for baryon violation] are generally inversely related to loop expansion parameters. So in any case where baryon violation is turned off after the phase transition, we should expect that the loop expansion will be under control. Our results only marginally validate this conclusion.

The casual reader who is interested only in our final numerical results should turn to Figs. 24–27 in Sec. VIII.

In Sec. II, we review the one-loop ring-improved potential and discuss how to power-count diagrams to find the dominant two-loop corrections for $g^4 \ll \lambda \ll g^2$. We will be led to adopt the formal power-counting rule $\lambda \sim g^3$ for the rest of the paper. In Sec. III, we warm up to the problem of two-loop thermal calculations by first concocting a scalar problem that is loosely analogous. We shall review the equivalence of various prescriptions for resummation of ring diagrams and we shall settle on one that implements resummation only for the effective three-dimensional theory obtained after heavy, nonstatic modes have been integrated out. In Sec. IV, we turn to the simplest gauge theory case—the Abelian Higgs model. As well as computing the two-loop potential near the phase transition, we isolate which contributions are important for shifting the VEV at the phase transition from its one-loop value. Section V is devoted to the contributions of chirally coupled fermions. In Sec. VI we discuss non-Abelian theories using SU(2) as an example, and we turn to the minimal standard model in particular in Sec. VII. Numerical results for the size of two-loop corrections in the minimal standard model are presented in Sec. VIII. Most of the results for diagrams contributing to the two-loop potential are collected in Appendix A. Ap-

pendix B gives derivations of the high-temperature expansions of some quantities discussed in the main text. Finally, Appendix C contains our criticism of the superdaisy approximation to the effective potential.

Throughout this paper we shall find it convenient to work exclusively in the Euclidean (imaginary time) formulation of thermal field theory. We shall conventionally refer to four-momenta with capital letters K and to their components with lowercase letters: $K = (k_0, \mathbf{k})$. All four-momenta are Euclidean, with discrete frequencies $k_0 = 2n\pi T$ for bosons and $(2n+1)\pi T$ for fermions, unless stated otherwise.

II. POWER COUNTING AND REVIEW

A. Pure scalar theory

The classical, zero-temperature Higgs potential is of the form

$$V_{\text{cl}}(\phi) = -\frac{1}{2}v^2\phi^2 + \frac{1}{4!}\lambda\phi^4. \quad (2.1)$$

For simplicity, let us temporarily ignore the gauge and fermion sectors and review the effect of finite temperature in a theory with a single, real scalar field. At high temperature T ($T \gg v$), there is an additional contribution to the scalar mass; the effective potential is approximately of the form

$$V_{\text{eff}}(\phi, T) \approx \frac{1}{2} \left[-v^2 + \frac{1}{24}\lambda T^2 \right] \phi^2 + \frac{1}{4!}\lambda\phi^4, \quad (2.2)$$

which is the same as the zero-temperature potential except that

$$v^2 \rightarrow v_{\text{eff}}^2 = -\frac{1}{24}\lambda T^2 + v^2. \quad (2.3)$$

The addition of the thermal mass term above is responsible for symmetry restoration at high temperature [15–17], and this approximation to the effective potential describes a second-order phase transition at $T_c^2 \approx 24v^2/\lambda$.

Diagrammatically, the thermal mass term in (2.2) arises from the quadratically divergent loop of Fig. 1. In the temperature-dependent piece of a quadratically divergent loop, the UV divergence is cut off at momenta of or-

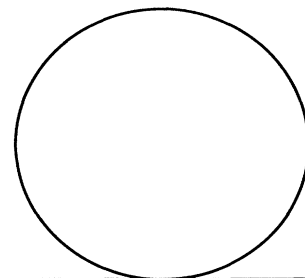


FIG. 1. Quadratically divergent loop giving rise to the thermal mass.

der T , and so Fig. 1 is of order λT^2 for temperatures large compared to the scalar mass.

The thermal mass above is simply the dominant term in a high-temperature expansion of the full finite-temperature one-loop potential. The temperature-

dependent piece of the full one-loop potential is simply the free energy of an ideal gas of scalar particles with mass $m^2(\phi) = V''_{\text{cl}}(\phi)$, which is the mass associated with fluctuations in the scalar field around a background field ϕ [17]:

$$V^{(1)}(\phi, T) = V_{\text{cl}}(\phi) + T \int \frac{d^3k}{(2\pi)^3} \ln(1 - \exp\{-\beta[k^2 + m^2(\phi)]^{1/2}\}) + (\text{one-loop zero-temperature result}) . \quad (2.4)$$

In the high-temperature limit $T \gg m(\phi)$,

$$V^{(1)}(\phi, T) = V_{\text{cl}}(\phi) + \text{const} + \frac{1}{24} m^2(\phi) T^2 - \frac{1}{12\pi} m^3(\phi) T + \mathcal{O}(m^4) \quad (2.5a)$$

$$= \text{const} + \frac{1}{2} \left[-v^2 + \frac{1}{24} \lambda T^2 \right] \phi^2 - \frac{1}{12\pi} \left[-v^2 + \frac{1}{2} \lambda \phi^2 \right]^{3/2} T + \frac{1}{4!} \lambda \phi^4 + \mathcal{O}(m^4) . \quad (2.5b)$$

The constants above are temperature dependent but ϕ independent. Such constants are not relevant to studying the mechanics of the phase transition, and we shall generally ignore them.

We have used the classical relation $m^2(\phi) = -v^2 + \frac{1}{2} \lambda \phi^2$ above; however, the effective value (2.3) of v^2 is quite different from its classical value at high tem-

perature ($T \gtrsim T_c$). It is therefore important to make the replacement (2.3) and use instead

$$m_{\text{eff}}^2(\phi) = -v^2 + \frac{1}{24} \lambda T^2 + \frac{1}{2} \lambda \phi^2 , \quad (2.6)$$

which inserted into (2.5a) yields the ring-improved one-loop potential [18–20]¹

$$V_{\text{ring}}^{(1)}(\phi, T) = \text{const} + \frac{1}{2} \left[-v^2 + \frac{1}{24} \lambda T^2 \right] \phi^2 - \frac{1}{12\pi} \left[-v^2 + \frac{1}{24} \lambda T^2 + \frac{1}{2} \lambda \phi^2 \right]^{3/2} T + \frac{1}{4!} \lambda \phi^4 + \mathcal{O}(m_{\text{eff}}^4) . \quad (2.7)$$

This potential sums the dominant contributions of the one-loop ring (or daisy) graphs shown in Fig. 2, where each quadratically divergent ring has been approximated by its high-temperature limit $\lambda T^2/24$. The substitution of v_{eff}^2 for v^2 corresponds to a resummation of the propagator as in Fig. 3. We shall treat this resummation more carefully and systematically in Sec. III.

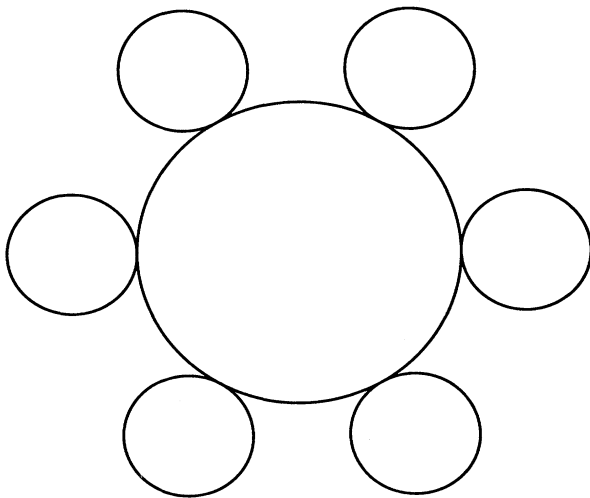


FIG. 2. A generic example of a one-loop ring (daisy) graph.

The potential (2.7) appears to describe a first-order phase transition, as shown in Fig. 4. At the temperature T_0 where the quadratic term vanishes, the potential is of the form $-b\lambda^{3/2}\phi^3 T + c\lambda\phi^4$ and has a minimum at nonzero $\phi \sim \sqrt{\lambda} T$. Just slightly above T_0 , the small quadratic term will generate a second minimum at $\phi=0$, indicating a first-order transition. The symmetry-breaking minimum at the phase transition, labeled ϕ_c in Fig. 4, will occur at a point where all three terms of the potential (2.7) are the same order of magnitude. One easily concludes that

$$\phi_c \sim \sqrt{\lambda} T, \quad -v_{\text{eff}}^2(T_c) \sim \lambda^2 T^2 . \quad (2.8)$$

In fact, the phase transition in the pure scalar theory is

$$(\text{---})^{-1} = (\text{---})^{-1} - \left[g^2 T^2 \text{ piece of } \bigcirc \right]$$

FIG. 3. Resummation of the propagator in the ring approximation.

¹This potential has an imaginary part at small ϕ . A physical interpretation may be found in Ref. [21].

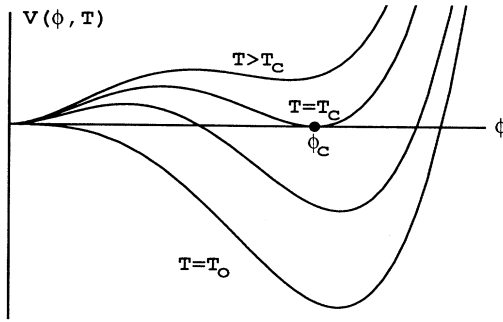


FIG. 4. Qualitative form of the potential as a function of temperature during a first-order phase transition. The potentials have been normalized to be zero at the origin.

known to be *second* order.² The conclusions from the previous paragraph cannot be trusted because higher-loop corrections to the one-loop ring-improved potential are large at ϕ_c . As discussed earlier, loops with quadratic UV divergences are of order λT^2 and are dominated by large momenta of order T . These $O(\lambda T^2)$ contributions are all absorbed by using ring-improved propagators. UV convergent loops (and the nondivergent pieces of quadratically divergent ones) are instead dominated by their infrared behavior. In Euclidean space, this means loop momenta are dominated by $k_0=0$ and $|\mathbf{k}| \sim m$. The dominant $k_0=0$ piece of the finite-temperature frequency sum $T \sum_{k_0}$ gives such loops a linear, rather than quadratic, dependence on T .³ Including a factor of $1/m_{\text{eff}}$ to make a dimensionless quantity, the cost of each loop is therefore $\lambda T/m_{\text{eff}}$.⁴ Now consider the loop expansion parameter $\lambda T/m_{\text{eff}}$ at the minimum $\phi_c \sim \sqrt{\lambda} T$ corresponding to the apparent first-order phase transition of the ring-improved one-loop potential (2.7). Equation (2.8) implies that $m_{\text{eff}}(\phi_c) \sim \lambda T$, and so the loop expansion parameter is of order 1, verifying that the ring-improved loop expansion cannot be trusted to distinguish between a first- and second-order phase transition in this model.

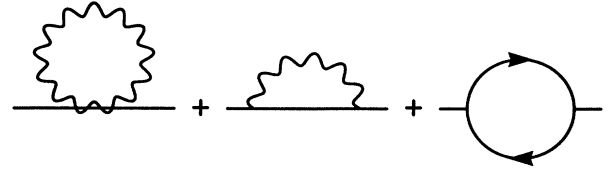


FIG. 5. Dominant contributions to the scalar thermal mass in gauge theories with fermions, in addition to Fig. 1.

B. Gauge theories

The situation is quite different when the gauge sector is included. As we now review, the first-order phase transition seemingly described by the ring-improved effective potential is associated with a *small* loop expansion parameter if the Higgs-boson mass is sufficiently small. The phase transition is therefore indeed first order, and the ring-improved loop expansion is a valid tool for studying it.

As in the pure scalar theory, there is a thermal contribution to the Higgs-boson mass. It is of the form

$$-v^2 \rightarrow -v_{\text{eff}}^2 = -v^2 + ag^2 T^2, \quad (2.9)$$

where ag^2 symbolizes a linear combination of the squared couplings in the theory. In the minimal standard model, for instance,

$$ag^2 \rightarrow \left[\lambda + \frac{9}{4}g_2^2 + \frac{3}{4}g_1^2 + 3g_y^2 \right] \frac{T^2}{12}, \quad (2.10)$$

where g_2 , g_1 , and g_y are the couplings for SU(2), U(1), and the top quark Yukawa interaction. (We shall always ignore all Yukawa couplings except for the top quark. See Sec. VII for coupling normalizations.) Diagrammatically, these contributions again arise from quadratically divergent loops, such as in Fig. 5.

The temperature dependence of the full finite-temperature one-loop potential may again be interpreted in terms of the free energy of an ideal gas. Now we must sum contributions from all the various particles in the theory with masses $m_i(\phi)$ induced by the background Higgs field ϕ :

$$\begin{aligned} V^{(1)}(\phi, T) &= V_{\text{cl}}(\phi) + \sum_i \pm n_i T \int \frac{d^3k}{(2\pi)^3} \ln(1 \mp \exp\{-\beta[k^2 + m_i^2(\phi)]^{1/2}\}) + (\text{one-loop zero-temperature result}) \\ &= V_{\text{cl}}(\phi) + \sum_i n_i \Delta V_i(\phi, T), \end{aligned} \quad (2.11)$$

where the sum is over all particle species i , n_i is the number of degrees of freedom associated with each species, and the upper (lower) sign is for bosons (fermions). The high-temperature limit $T \gg m_i(\phi)$ is [17]

²See any textbook on critical phenomena. Concerning the order of the transition in the gauged case, see Ref. [22] for an analysis more generally applicable than what we shall review below. For recent comments on this issue, see Ref. [30].

³An early discussion of this power counting may be found in Ref. [16].

⁴Loops which are logarithmically UV divergent may cost a factor of $(\lambda T/m_{\text{eff}})\ln(T/m_{\text{eff}})$. We shall ignore the logarithms when power counting.

$$\begin{aligned}\Delta V_i(\phi, T) &= \text{const} + \frac{1}{24} m_i^2(\phi) T^2 - \frac{1}{12\pi} m_i^3(\phi) T + \mathcal{O}(m_i^4) \quad (\text{bosons}), \\ \Delta V_i(\phi, T) &= \text{const} + \frac{1}{48} m_i^2(\phi) T^2 + \mathcal{O}(m_i^4) \quad (\text{fermions}).\end{aligned}\tag{2.12}$$

As before, we shall generally ignore the ϕ -dependent constants indicated by “const” above.

For gauge bosons and the top quark, $m_i(\phi)$ is proportional to $g\phi$ where g is the appropriate coupling. Ignoring the Higgs contribution for now, the high-temperature expansion of the one-loop potential is then schematically of the form

$$V^{(1)}(\phi, T) \approx \frac{1}{2} (-v^2 + ag^2 T^2) \phi^2 - bg^3 \phi^3 T + \frac{1}{4!} \lambda \phi^4, \tag{2.13}$$

where, for the standard model,

$$bg^3 \phi^3 T \rightarrow [6M_W^3(\phi) + 3M_Z^3(\phi)] \frac{T}{12\pi} = \left[\frac{3}{4} g_2^3 + \frac{3}{8} (g_1^2 + g_2^2)^{3/2} \right] \phi^3 \frac{T}{12\pi}. \tag{2.14}$$

Because of the ϕ^3 term, the potential (2.13) describes a first-order phase transition.

As before, we can ring improve the one-loop potential to sum one-loop ring diagrams such as Fig. 6. In Euclidean space, the small, hard loops are quadratically divergent and contribute a thermal mass of order $g^2 T^2$ to the A_0 polarization of the gauge fields. This is the usual Debye mass, and the ring improvement is implemented by incorporating it into $M(\phi)$ for that polarization [20]. For instance, the W contribution to the cubic term (2.14) changes from

$$6M_W^3(\phi) \frac{T^2}{12\pi} \quad \text{to} \quad [4M_W^3(\phi) + 2M_{LW}^3(\phi)] \frac{T^2}{12\pi}, \tag{2.15}$$

where

$$M_W^2(\phi) = \frac{1}{4} g_2^2 \phi^2, \quad M_{LW}^2(\phi) = \frac{1}{4} g_2^2 \phi^2 + \frac{1}{6} g_2^2 T^2. \tag{2.16}$$

For Euclidean frequency $k_0=0$, which dominates the infrared (IR) behavior of loops, we shall refer to the A_0 po-

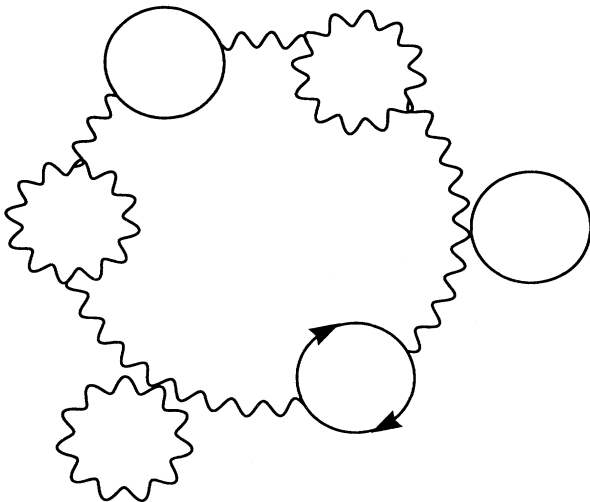


FIG. 6. Generic one-loop ring diagram in a gauge theory with fermions.

larization as the *longitudinal* polarization and the other two polarization perpendicular to the four-momentum as the transverse polarizations. The ring improvement of the terms arising from the Z are more complicated due to mixing with the photon [20], and we leave explicit formulas for Sec. VII.

We now estimate the order of magnitude of parameters associated with the phase transition. Consider the schematic form of the potential (2.13). (The ring improvement will not modify the following order-of-magnitude estimates). As in the scalar case, the nonzero minimum at the phase transition occurs when all three terms are roughly the same order of magnitude, which yields

$$\phi_c \sim \frac{g^2}{\lambda} T, \quad -v_{\text{eff}}^2 \sim \frac{g^6}{\lambda} T^2. \tag{2.17}$$

Table I shows the order of magnitude of several other parameters. Of particular interest is the loop expansion parameter for loops involving massive gauge bosons; it is order λ/g^2 . We shall formally assume $\lambda \ll g^2$ (that is, $m_H \ll M_W$ at zero temperature) so that the loop expansion is well-behaved. (In Sec. III, we shall discuss in more detail why the *vector* loop expansion parameter is the relevant one for our calculation.) Furthermore, to justify our ubiquitous high-temperature expansion $T \gg M$ and m , Table I shows that we must also assume $g^4 \ll \lambda$.

Assuming $g^4 \ll \lambda \ll g^2$, our goal is to consistently compute the leading correction to the ring-improved one-loop potential. It is cumbersome to compare orders of magnitude of various corrections when there are two coupling constants g and λ . Fortunately, the power counting can be simplified by formally taking

$$\lambda \sim g^3, \tag{2.18}$$

which is at the geometric center of the range $g^4 \ll \lambda \ll g^2$ under consideration. This simplification seems to always order the relative size of corrections in a way that is consistent over this entire range of λ . We henceforth always assume $\lambda \sim g^3$ unless otherwise stated. The simplified power counting is shown in the far-right column of Table I. Note that the vector loop expansion

TABLE I. Orders of magnitude of parameters in the $\phi \neq 0$ vacuum at the phase transition. The far right column gives the simplified power-counting rules, which assume $\lambda \sim g^3$. The entry for the two-loop correction to the potential refers to the dominant ϕ -dependent corrections.

		$\lambda \sim g^3$
Scalar mass	$\phi \sim (g^3/\lambda)T$	T
Transverse vector mass	$m \sim (g^3/\sqrt{\lambda})T$	$g^{3/2}T$
Vector Debye mass	$M \sim (g^4/\lambda)T$	gT
Vector loop expansion parameter	$(M_L^2 - M^2)^{1/2} \sim gT$	gT
Scalar loop expansion parameter	$g^2T/M \sim \lambda/g^2$	g
	$\lambda T/m \sim (\lambda/g^2)^{3/2}$	$g^{3/2}$
	$(T_c - T_0)/T_c \sim g^4/\lambda$	g
Barrier in V between minima	$V \sim (g^{12}/\lambda^3)T^4$	g^3T^4
Two-loop correction to potential	$(g^2T/M)V \sim (g^{10}/\lambda^2)T^4$	g^4T^4

parameter is g (rather than g^2 , as it would be at zero temperature) and that the Debye mass and the transverse vector mass are formally the same order of magnitude.

C. Multiple loops and IR disasters

In studies of high-temperature QCD, it is well known that the perturbative computation of the free energy breaks down at three loops because of infrared divergences associated with static ($k_0=0$), transverse gluons [23]. Though the longitudinal gluons pick up a Debye mass of order gT at one loop, as discussed earlier, the transverse gluons do not. These IR divergences are interpreted as a sign that the transverse gluons must have a mass of order g^2T which is not perturbatively calculable, corresponding to a finite screening length for static, magnetic fields in the plasma. The uncertainty in the free energy due to the incalculability of this effect is order g^6T^4 .⁵

The situation is different in a spontaneously broken theory because the gauge bosons corresponding to broken symmetries are not massless. In pure electroweak theory, for example, the transverse W and Z bosons are massive in the symmetry-breaking minimum at the phase transition. One can compute to *any* order of perturbation theory in this minimum without infrared singularities. (A perturbative expansion is still not useful, of course, unless the loop expansion parameter is small.) However, there is still a limit to how well the phase transition can be studied, because determining the temperature of the phase transition requires comparing the free energy of the asymmetric $\phi \neq 0$ minimum with the symmetric $\phi = 0$ one, and all the familiar problems of high-temperature QCD arise in the symmetric minimum. The calculation of the free energy at $\phi = 0$ breaks down at three loops and

has an uncertainty of order g^6T^4 ; there is therefore little point in computing the free energy of the asymmetric vacuum to any better accuracy. At the phase transition, the typical size of each of the three terms in (2.13) is g^3T^4 and the size of n -loop corrections are suppressed by $(g^2T/M)^{n-1}$, giving $g^{n+2}T^4$. So there is no point computing the free energy beyond three loops near the asymmetric vacuum. Being unadventurous, we shall limit ourselves to computing two-loop corrections.

In the *full* standard model, IR singularities are encountered even in the asymmetric vacuum because the electroweak sector couples to the top quark, which couples to transverse gluons. In the asymmetric vacuum, this problem does not manifest until five-loop contributions to the potential are considered.

III. WARMING UP WITH A SCALAR TOY MODEL

We now want to proceed to compute the dominant two-loop contributions to the potential. To introduce the basic computational method, we wish to start with as simple an example as possible: a pure scalar theory of a single, real field. Sadly, we saw in the last section that the loop expansion cannot be trusted to study the phase transition in this model, because the loop expansion parameter $\lambda T/m_{\text{eff}}(\phi_c)$ is order 1. However, there is no reason we cannot compute the effective potential at larger values of ϕ where $m_{\text{eff}}(\phi)$ is larger so that the loop expansion parameter is smaller. This region of the potential has nothing to do with the phase transition in this model, but it provides a simple example of the computations and approximations that we later implement in gauged models. We shall take a classical Higgs potential of the form

$$V_{\text{cl}}(\phi) = -\frac{1}{2}v^2\phi^2 + \frac{1}{4!}g^2\phi^4 \quad (3.1)$$

and shall study the potential for ϕ of order

$$\phi \sim T \quad (3.2)$$

at temperatures T near the critical temperature T_c . This is supposed to be analogous to the $\lambda \sim g^3$ gauge theory discussed in the last section insofar as (1) there is a zero-temperature loop expansion parameter called g^2 , and (2) we examine the potential at $\phi \sim T$ (see Table I). The effective scalar mass is then of order gT and the loop ex-

⁵We remind the reader of a simple mnemonic for this result. The only scale in the effective three-dimensional theory, which is the source of the IR divergences, is g^2T . So the free energy of the three-dimensional theory, which will be incalculable by perturbation theory, is order $(g^2T)^3$ by dimensional analysis. The relation between the four-dimensional and three-dimensional free energies is a factor of T , giving g^6T^4 .

pansion parameter is order $g^2 T/m \sim g$, both analogous to the vector mass and vector loop expansion parameter in Table I. We have named the scalar self-coupling g^2 in the toy model both to emphasize this analogy and to avoid confusion with our $\lambda \sim g^3$ convention used in the gauged models. We hope that the reader's benefit from seeing the techniques first presented in a simple model will outweigh any confusion inherent in the temporary change of conventions. Orders of magnitude are summarized in Table II.

Let us apply our earlier review of power counting to estimate the two-loop contribution to the potential. Ignoring quadratically divergent loops, which will be absorbed by ring improvement, the dominant two-loop contribution should be order $g^2 T^2 m^2$, where there is an explicit power of g^2 , an explicit power of T for each loop, and then m^2 by dimensional analysis. Since $m \sim gT$, the two-loop contribution is equivalently order $g^4 T^4$. When computing the two-loop potential, we shall always drop any contributions smaller than $O(g^4 T^4)$. In the region of ϕ under study, the contributions dropped are of the same order as three- and higher-loop contributions, and so there is no point in retaining them in a two-loop calculation.

A. The one-loop result without resummation

We shall leave the analysis of resumming rings for Secs. III C and III D. For now, we focus on the details of the unimproved loop expansion in this model and start by carefully examining one-loop results. We need to keep terms to order $g^4 T^4$, which requires one higher order in the high-temperature expansion (2.5a) discussed in the Introduction. At this order the one-loop potential receives UV infinite contributions from usual zero-temperature divergences, and so we must confront regularization and counterterms. We shall regularize all our calculations using dimensional regularization in $4-2\epsilon$ di-

TABLE II. Orders of magnitude of parameters in the scalar toy model for $\phi \sim T$ and $T \sim T_c$. The entry for the two-loop correction to the potential refers to the dominant ϕ -dependent corrections.

Scalar toy model	
By assumption:	$\phi \sim T$
Effective mass at ϕ	$m(\phi) \sim gT$
Debye mass	$\sim gT$
Loop expansion parameter	$g^2 T/m(\phi) \sim g$
Two-loop correction to potential	$\sim g^4 T^4$

mensions. Computing counterterms to one-loop order, one finds that the bare potential expressed in terms of the renormalized coupling constants is

$$\begin{aligned} V_{\text{bare}}(\phi) &= -\frac{1}{2} v_{\text{bare}}^2 \phi_{\text{bare}}^2 + \frac{1}{4!} g_{\text{bare}}^2 \phi_{\text{bare}}^4 \\ &= -\frac{1}{2} Z_1 v^2 \phi^2 + \frac{1}{4!} \mu^{2\epsilon} Z_2 g^2 \phi^4, \end{aligned} \quad (3.3)$$

$$Z_1 = 1 + \frac{1}{32\pi^2} g^2 \frac{1}{\epsilon} + O(g^4). \quad (3.4a)$$

$$Z_2 = 1 + \frac{3}{32\pi^2} g^2 \frac{1}{\epsilon} + O(g^4). \quad (3.4b)$$

μ is the arbitrary renormalization scale. We shall use modified minimal subtraction scheme ($\overline{\text{MS}}$) regularization, which, we remind the reader, corresponds to performing minimal subtraction (MS) and then changing scales to $\bar{\mu}$ by the substitution

$$\mu = \bar{\mu} \left[\frac{e^{\gamma_E}}{4\pi} \right]^{1/2}, \quad (3.5)$$

where γ_E is Euler's constant.

The next term in the high-temperature expansion of the one-loop potential is well known (but we shall review the derivation in Sec. III D) [17]:

$$\mu^{2\epsilon} \mathcal{V}_{\mathcal{R}}^{(1)}(\phi) = \mu^{2\epsilon} V_{\text{bare}}(\phi) + J[m(\phi)], \quad (3.6)$$

$$\begin{aligned} J(m) &= \frac{1}{2} \mu^{2\epsilon} \mathcal{F}_{\mathcal{R}} \ln(K^2 + m^2) \\ &= \text{const} + \frac{1}{24} m^2 T^2 - \frac{1}{12\pi} m^3 T - \frac{1}{64\pi^2} m^4 \left[\frac{1}{\epsilon} + \ln \left[\frac{\bar{\mu}^2}{T^2} \right] - 2c_B \right] + O(m^6/T^2) + O(\epsilon), \end{aligned} \quad (3.7)$$

where

$$m^2(\phi) = -v^2 + \frac{1}{2} g^2 \mu^{2\epsilon} \phi^2, \quad c_B = \ln(4\pi) - \gamma_E, \quad (3.8)$$

and the integral-summation sign above is shorthand for the Euclidean integration

$$\mathcal{F}_{\mathcal{R}} \rightarrow T \sum_{k_0} \int \frac{d^{3-2\epsilon} k}{(2\pi)^{3-2\epsilon}}. \quad (3.9)$$

The sum is over $k_0 = 2\pi nT$ for all integers n .

The divergences in $J(m)$ cancel against the counterterms in $V_{\text{bare}}(\phi)$. The reader should note that our

definition of $J(m)$ includes *both* the temperature-dependent and zero-temperature contributions.⁶ Note also that $\overline{\text{MS}}$ regularization does not get rid of all factors of γ_E and $\ln(4\pi)$ as it would at zero temperature. The subscript \mathcal{R} above refers to the absence of resummation.

⁶One often sees only the temperature-dependent piece in the literature, which has an $m^4 \ln(m^2/T^2)$ term, which is not analytic in m^2 . It is important to realize that in the full result, which includes the zero-temperature contribution, the only term not analytic in m^2 is the $m^3 T$ term.

B. The two-loop result without resummation

The two-loop diagrams are shown in Fig. 7, where the heavy dots represent one-loop, zero-temperature counterterms. The propagators use the mass (3.8) appropriate in the presence of the background field ϕ , and we shall usually refer to $m^2(\phi)$ simply as m^2 . The crosses in the diagrams represent explicit factors of the background field ϕ at vertices.

Figure 7(a) is the most straightforward of the two-loop diagrams, giving a contribution to the effective potential of

$$\mu^{2\epsilon} \mathcal{V}_R^{(a)} = \frac{1}{8} g^2 [I(m)]^2, \quad (3.10)$$

where

$$I(m) = \mu^{2\epsilon} \int \int_K \frac{1}{K^2 + m^2}. \quad (3.11)$$

$I(m)$ is related to $J(m)$ of (3.6) by $I(m) = m^{-1} dJ/dm$, and so its high-temperature expansion is

$$\begin{aligned} I(m) = & \frac{1}{12} T^2 - \frac{1}{4\pi} mT - \frac{1}{16\pi^2} m^2 \left[\frac{1}{\epsilon} + \ln \left[\frac{\bar{\mu}^2}{T^2} \right] - 2c_B \right] \\ & + O(m^4/T^2) + \epsilon \nu_\epsilon \frac{1}{12} T^2 + O(\epsilon mT), \end{aligned} \quad (3.12)$$

where we have now explicitly shown the leading term of order ϵ . Though it will appear in results for individual diagrams, it turns out that

$$\nu_\epsilon = \ln \left[\frac{\bar{\mu}^2}{T^2} \right] + 2\gamma_E - 2 \ln 2 - 2 \frac{\zeta'(2)}{\zeta(2)} \quad (3.13)$$

is an unimportant constant because it will cancel in our final result. (A sketch of the derivation of ν_ϵ may be found in Sec. III D. ζ is the Riemann zeta function.) Using the expansion (3.12) in the contribution (3.10) to the potential, and keeping terms only up to $O(g^4 T^4)$,

$$\mu^{2\epsilon} \mathcal{V}_R^{(a)} = \text{const} - \frac{1}{48 \times 4\pi} g^2 m T^3 - \frac{1}{48(4\pi)^2} g^2 m^2 T^2 \left[\frac{1}{\epsilon} + \nu_\epsilon + \ln \left[\frac{\bar{\mu}^2}{T^2} \right] - 2c_B - 6 \right] + O(g^5 T^4). \quad (3.14)$$

(When we later address the resummation of rings, we shall find that the first term, which is order $g^3 T^4$, is absorbed by the resummation.)

Figure 7(b) is more interesting because it is logarithmically divergent in the three-dimensional theory (that is, when all loop frequencies k_0 are set to zero). As a result, it generates a logarithmic dependence on the mass $m(\phi)$, unlike the one-loop contribution or Fig. 7(a). As we shall see when we later return to gauge theories, it is such loga-

arithmic terms which are almost solely responsible, at the order under consideration, for modifying the VEV at the phase transition from its one-loop value.

Turning to specifics, the contribution of Fig. 7(b) is

$$\mu^{2\epsilon} \mathcal{V}_R^{(b)} = -\frac{1}{12} g^4 \mu^{2\epsilon} \phi^2 H(m), \quad (3.15)$$

where

$$H(m) = \mu^{4\epsilon} \int \int_P \int \int_Q \frac{1}{(P^2 + m^2)(Q^2 + m^2)[(P+Q)^2 + m^2]}. \quad (3.16)$$

The high-temperature limit of H has been evaluated by Parwani [24], who finds

$$H(m) = \frac{1}{64\pi^2} T^2 \left[\frac{1}{\epsilon} + \nu_\epsilon + \ln \left[\frac{\bar{\mu}^2}{T^2} \right] + 2 \ln \left[\frac{T^2}{m^2} \right] + 2 - c_H \right] + O(m^2) + O(\epsilon T^2), \quad (3.17)$$

where

$$c_H \approx 5.3025 \quad (3.18)$$

is a numerical constant which can be expressed in terms of double definite integrals of elementary functions. (See Ref. [24] for details.) Substitution into (3.15) gives

$$\mu^{2\epsilon} \mathcal{V}_R^{(b)} = \frac{1}{48(4\pi)^2} g^4 \mu^{2\epsilon} \phi^2 T^2 \left[-\frac{1}{\epsilon} - \nu_\epsilon - \ln \left[\frac{\bar{\mu}^2}{T^2} \right] - 2 \ln \left[\frac{T^2}{m^2} \right] - 2 + c_H \right] + O(g^5 T^4). \quad (3.19)$$

Note the promised presence of $\ln[m(\phi)]$.

The two counterterm graphs [Figs. 7(c) and 7(d)] give

$$\mu^{2\epsilon} V_R^{(c)} = -\frac{1}{4(4\pi)^2} g^2 v^2 I(m) \frac{1}{\epsilon} = \text{const} + O(g^5 T^4), \tag{3.20}$$

$$\mu^{2\epsilon} V_R^{(d)} = \frac{3}{8(4\pi)^2} g^4 \mu^{2\epsilon} \phi^2 I(m) \frac{1}{\epsilon} = \frac{3}{96(4\pi)^2} g^4 \mu^{2\epsilon} \phi^2 T^2 \left[\frac{1}{\epsilon} + \iota_\epsilon \right] + O(g^5 T^4). \tag{3.21}$$

Combining the results of this subsection with (3.6) yields the unimproved two-loop potential:

$$\begin{aligned} \mu^{2\epsilon} V_R^{(2)} = & \text{const} - \frac{1}{48 \times 4\pi} g^2 m T^3 + \frac{1}{2} \left\{ \left[-v^2(T) + \frac{1}{24} g^2(T) T^2 \right] - \frac{1}{(4\pi)^2} c_B g^2 v^2 \right. \\ & \left. - \frac{1}{24(4\pi)^2} g^4 T^2 \left[2 \ln \left[\frac{T^2}{m^2} \right] - 1 - c_B - c_H \right] \right\} \phi^2 \\ & - \frac{1}{12\pi} m^3 T + \frac{1}{4!} \left[g^2(T) + \frac{3}{(4\pi)^2} c_B g^4 \right] \phi^4 + O(g^5 T^4), \end{aligned} \tag{3.22}$$

where

$$m^2 = -v^2 + \frac{1}{2} g^2 \phi^2, \tag{3.23}$$

$$g^2(T) = g^2 - \frac{3}{32\pi^2} g^4 \ln \left[\frac{\bar{\mu}^2}{T^2} \right] + \dots, \tag{3.24}$$

$$v^2(T) = v^2 \left[1 - \frac{1}{32\pi^2} g^2 \ln \left[\frac{\bar{\mu}^2}{T^2} \right] + \dots \right]. \tag{3.25}$$

As it should be, the result is invariant under the renormalization group to the order we have computed. We have chosen to write the answer in terms of the running couplings⁷ $g^2(T)$ and $v^2(T)$. (At this order we need not worry about the anomalous scaling of ϕ .) The physical scales in this problem are m and T , and so, when evaluating (3.22) in practice, we should choose the renormalization scale $\bar{\mu}$ to avoid producing large logarithmic enhancements, $\ln(\bar{\mu}/T)$ or $\ln(\bar{\mu}/m)$, of yet higher-order corrections. Fortunately, since $m \sim gT$, m and T are not drastically different scales. The difference between $g^2(T)$ and $g^2(m)$ is of order $g^4 \ln g$ and is indeed small, and so $\bar{\mu} \sim T$ and $\bar{\mu} \sim m$ are both adequate choices. We chose to write (3.22) in terms of $g^2(T)$ instead of $g^2(m)$, but this

choice is merely convention and lacks physical significance.

C. Resummation: Method I

How do I resum thee? Let me count the ways.

We now want to implement the resummation of the dominant parts of ring diagrams by replacing $m^2(\phi)$ in our propagators by $m_{\text{eff}}^2(\phi)$ as defined in (2.6) to include the thermal contribution to the mass. Parwani [24] (who has computed the subleading correction to the scalar mass at high temperatures) uses one method for doing this systematically and consistently. Rewrite the bare potential (3.3) as

$$\begin{aligned} V_{\text{bare}}(\phi) = & \frac{1}{2} Z_1 \left[-v^2 + \frac{1}{24} g^2 T^2 \right] \phi^2 \\ & + \frac{1}{4!} \mu^{2\epsilon} Z_2 g^2 \phi^4 - \frac{1}{48} Z_1 g^2 T^2 \phi^2, \end{aligned} \tag{3.26}$$

where the thermal mass term has simply been added in and subtracted out again so that nothing is changed. But now interpret the first term as part of the *unperturbed* Lagrangian \mathcal{L}_0 and treat the last term as a perturbation. (We shall loosely refer to the last term as the thermal “counterterm,” but we have not in fact changed the renormalization prescription from the usual zero-temperature one.) Nothing has changed if all orders of

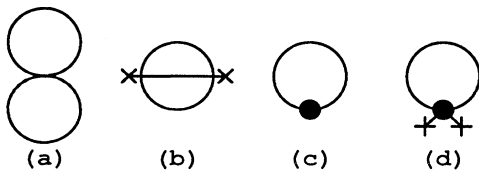


FIG. 7. Two-loop contributions to the potential of the scalar toy model.

⁷These couplings are run with the usual zero-temperature renormalization group and do not represent the use of any sort of temperature-dependent renormalization-group equations.

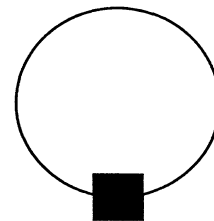


FIG. 8. Two-loop contribution involving the thermal counterterm.

perturbation theory are summed. However, order by order, the $g^2 T^2$ pieces of quadratically divergent subloops now cancel against diagrams involving the thermal counterterm; the new perturbative expansion is controlled by the convergent-loop expansion parameter $g^2 T/m$.

In the case at hand, this resummation replaces $m(\phi)$ by

$$m_{\text{eff}}(\phi) = -v^2 + \frac{1}{2}g^2\mu^{2\epsilon}\phi^2 + \frac{1}{24}g^2T^2 \quad (3.27)$$

in our previous calculations of contributions to the two-loop potential⁸ and introduces the new diagram of Fig. 8. The box represents the thermal counterterm—the interaction generated by the last term in (3.26). Figure 8 gives

$$\begin{aligned} \mu^{2\epsilon}V^{(\text{CT})} &= -\frac{1}{48}g^2T^2I(m_{\text{eff}}) \\ &= \text{const} + \frac{1}{48 \times 4\pi}g^2m_{\text{eff}}T^3 + \frac{1}{48(4\pi)^2}g^2m_{\text{eff}}^2T^2 \left[\frac{1}{\epsilon} + \ln \left[\frac{\bar{\mu}^2}{T^2} \right] - 2c_B \right] + O(g^5T^4). \end{aligned} \quad (3.28)$$

Replacing $m \rightarrow m_{\text{eff}}$ in the original two-loop contributions (3.14), (3.19)–(3.21), and combining with (3.28) above now gives

$$\begin{aligned} V^{(2)} &= \text{const} + \frac{1}{2} \left\{ \left[-v^2(T) + \frac{1}{24}g^2(T)T^2 \right] - \frac{1}{(4\pi)^2}c_B g^2 v^2 - \frac{1}{24(4\pi)^2}g^4T^2 \left[2 \ln \left[\frac{T^2}{m_{\text{eff}}^2} \right] - 1 - c_B - c_H \right] \right\} \phi^2 \\ &\quad - \frac{1}{12\pi}m_{\text{eff}}^3T + \frac{1}{4!} \left[g^2(T) + \frac{3}{(4\pi)^2}c_B g^4 \right] \phi^4 + O(g^5T^4). \end{aligned} \quad (3.29)$$

Compare this to the unimproved result (3.22). As promised earlier, the $O(g^2mT^3)$ term of the figure-eight diagram (3.14) has disappeared, canceled by the thermal counterterm diagram (3.28). The original $O(g^2mT^3)$ contribution arose from taking the subleading $O(mT)$ contribution of one-loop integral times the leading $O(T^2)$ piece of the other, and the latter is precisely what resummation is intended to absorb.

D. Resummation: Method II

The implementation of resummation above is a little less natural for gauged theories. The scalar ring diagram in Fig. 1 is independent of momentum, whereas the quadratically divergent diagrams of Fig. 6 for gauged theories are not. Moreover, the polarization dependence of these g^2T^2 contributions to the vector self-energy $\Pi_{\mu\nu}(K)$ also depends on momentum [23] and is simple only in limits such as $K \rightarrow 0$, where only the contribution to $\Pi_{00}(0)$ is nonzero.⁹ Having computed the leading contribution to the self-energy $\Pi(K)$, should one resum the vector propagator $G_0(K)$ as $1/[G_0^{-1}(K) + \Pi(K)]$ or $1/[G_0^{-1}(K) + \Pi(0)]$ or something else? The answer is

that it does not matter. Resummation only affects perturbative expansions when Π cannot be treated as a perturbation to the inverse propagator G_0^{-1} . This happens only when $K^2 \ll T^2$, in which case $\Pi(K) \approx \Pi(0)$.

To see more explicitly that resummation is irrelevant when $\Pi \ll G_0^{-1}$, consider $K^2 \sim T^2$. Then $\Pi(K) \sim g^2T^2$ and $G_0^{-1}(K) \sim T^2$. The resummed propagator for $K^2 \sim T^2$ can then be expanded perturbatively in powers of $\Pi G_0 \sim g^2$. For example, the resummed propagator of the previous section may be expanded as¹⁰

$$\begin{aligned} \frac{1}{K^2 + m^2 + ag^2T^2} &= \frac{1}{K^2 + m^2} - \frac{ag^2T^2}{(K^2 + m^2)^2} \\ &\quad + \frac{(ag^2T^2)^2}{(K^2 + m^2)^3} - \dots \end{aligned} \quad (3.30)$$

The n th term is order g^{2n} . Every term, except the first, gives contributions (inside any diagram) that cancel *order-by-order* against insertions of the thermal counterterm, as in Fig. 9. So resummation for $K^2 \sim T^2$ has no effect on the perturbative expansion of the final result. (We shall see this even more explicitly in a moment by recomputing the two-loop potential in our scalar toy

⁸This substitution may be made directly in the results of Secs. III A and III B except for the final formula (3.22) because the expansion (3.8) of $m^2(\phi)$ was used when putting the result in its final form.

⁹We emphasize that we are working in Euclidean space, and so by $\Pi(0)$ we always mean $\Pi(k_0=0, \mathbf{k} \rightarrow 0)$ since k_0 is discrete. If one analytically continues k_0 to real time and takes instead the limit $\Pi(k_0 \rightarrow 0, \mathbf{k}=0)$, the limit is completely different, giving the plasma mass for propagating waves \mathbf{A} rather than the Debye mass for static electric potentials A_0 .

¹⁰Since $m^2 \sim g^2T^2$, we could expand the powers of m as well, but we have not bothered to do so.

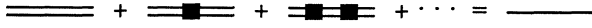


FIG. 9. Cancellations of resummation and thermal counter-terms.

model using a different resummation prescription.)

The circumstance where resummation is relevant is the infrared region $K^2 \lesssim (gT)^2$ where $\Pi \sim G_0^{-1}$. Then all terms in (3.30) are the same order. Any resummation prescription which approximates $\Pi(0)$ in the infrared region will do. In general, any resummation $1/[G_0^{-1}(K) + \mathcal{P}(K)]$ will work if (1) $\mathcal{P}(K) \approx \Pi(0)$ when $K^2 \lesssim (gT)^2$ and (2) $\mathcal{P}(K) \lesssim g^2 T^2$ for general K .

Since $K^2 \lesssim (gT)^2$ implies $k_0 = 0$ in Euclidean space, the resummation prescription for $k_0 \neq 0$ modes is irrelevant [as long as condition (2) is met]. Since resummation is an infrared phenomena, we find it convenient to adopt the following point of view, in the spirit of decoupling and the renormalization group. When computing the effective potential, first integrate out all of the heavy $k_0 \neq 0$ modes (ignoring the issue of resummation) to obtain an effective, three-dimensional theory of the $k_0 = 0$ modes. This will generate the thermal mass terms as well as other interactions induced by the heavy modes, which we compute to the desired order in perturbation theory. Only then do we finally integrate the $k_0 = 0$ modes after deciding on a sensible partition of the effective three-

dimensional Lagrangian into an unperturbed piece \mathcal{L}_0 , containing the thermal mass terms, and a perturbative piece. In the language of the previous paragraphs, this corresponds to choosing a resummed propagator $1/(G_0^{-1} + \mathcal{P})$ with

$$\mathcal{P}(K) = \begin{cases} \bar{\Pi}(0), & k_0 = 0, \\ 0, & k_0 \neq 0, \end{cases} \quad (3.31)$$

where $\bar{\Pi}(0)$ is the dominant $\mathcal{O}(g^2 T^2)$ term of $\Pi(0)$. [One could alternatively replace $\bar{\Pi}(0)$ by the full $\Pi(0)$ calculated to some order in perturbation theory, but perturbative changes to \mathcal{P} have no effect on the perturbation expansion.]

Though resumming only the $k_0 = 0$ modes sounds a little more cumbersome than resumming all the modes, we find it algebraically simpler in the gauge theory case because $1/[G_0^{-1}(K) + \Pi(K)]$ and $1/[G_0^{-1}(K) + \bar{\Pi}(0)]$ turn out to have more complicated polarization dependence for $k_0 \neq 0$ than for $k_0 = 0$. We also find it conceptually simpler to apply resummation only to the modes which require it.

As a paradigm for splitting calculations into heavy $k_0 \neq 0$ modes and light $k_0 = 0$ modes, and to emphasize the fact that masses (or self-energies) may be treated perturbatively for heavy modes but not for light ones, we shall briefly sketch the derivation of the high-temperature expansion (3.12) of $I(m)$ from its definition (3.11):

$$\begin{aligned} I(m) &= \mu^{2\epsilon} T \int \frac{d^{3-2\epsilon} k}{(2\pi)^{3-2\epsilon}} \frac{1}{k^2 + m^2} + 2\mu^{2\epsilon} T \sum_{n=1}^{\infty} \int \frac{d^{3-2\epsilon} k}{(2\pi)^{3-2\epsilon}} \frac{1}{(2\pi n T)^2 + k^2 + m^2} \\ &= \mu^{2\epsilon} T \int \frac{d^{3-2\epsilon} k}{(2\pi)^{3-2\epsilon}} \frac{1}{k^2 + m^2} + 2\mu^{2\epsilon} T \sum_{l=0}^{\infty} \sum_{n=1}^{\infty} \int \frac{d^{3-2\epsilon} k}{(2\pi)^{3-2\epsilon}} \frac{(-)^l m^{2l}}{[(2\pi n T)^2 + k^2]^{l+1}} \\ &= \frac{\Gamma(-\frac{1}{2} + \epsilon)}{(4\pi)^{3/2}} \left[\frac{4\pi\mu^2}{m^2} \right]^\epsilon m T + \frac{T^2}{(4\pi)^{1/2}} \left[\frac{\mu^2}{\pi T^2} \right]^\epsilon \sum_{l=0}^{\infty} \frac{\Gamma(l - \frac{1}{2} + \epsilon)}{\Gamma(l+1)} (-)^l \left[\frac{m}{2\pi T} \right]^{2l} \zeta(2l - 1 + 2\epsilon) \\ &= \frac{1}{12} T^2 - \frac{1}{4\pi} m T - \frac{1}{16\pi^2} m^2 \left[\frac{1}{\epsilon} + \ln \left[\frac{\bar{\mu}^2}{T^2} \right] - 2c_B \right] + T^2 \sum_{l=2}^{\infty} \left[\frac{-m^2}{4\pi^2 T^2} \right]^l \frac{(2l-3)!!}{(2l)!!} \zeta(2l-1) + \mathcal{O}(\epsilon), \quad (3.32) \end{aligned}$$

where ζ is the Riemann zeta function. In the first line we split the calculation into $k_0 = 0$ and $k_0 \neq 0$ modes; in the second line we expand the heavy modes in powers of m^2 ; in the third we first evaluate the momentum integrals and then sum over n ; and in the last line we take the $\epsilon \rightarrow 0$ limit. [This derivation may be used to obtain the constant ι_ϵ of (3.13).] The point of this example lies not in the mathematical details but in the fact that, in the sum over heavy modes, we are able to treat m^2 as a perturbation; the expansion of the integrand in m^2 for these modes is equivalent to the high-temperature expansion in m^2/T^2 . The $k_0 = 0$ term, on the other hand, produces the only term not analytic in m^2 —the mT term at $\mathcal{O}(\epsilon^0)$.

[One may now also obtain the high-temperature expansion (3.7) of $J(m)$ by using $I(m) = m^{-1} dJ/dm$.]

We now demonstrate how the new method of resummation works in our scalar toy model. For the scalar case, the new method will seem more convoluted than the previous one, but we find it simpler to use when we compute in gauge theories.

The resummation of the setting-sun diagram of Fig. 7(b) is shown in Fig. 10. The $k_0 \neq 0$ lines are marked “heavy” and the $k_0 = 0$ lines marked “zero.” The double lines represent resummed propagators. This expression may be simplified by realizing that the second term is order $g^5 T^4$ and hence ignorable; this term is of the form

(leaving out ϵ 's to avoid clutter)

$$\begin{aligned}
 & \frac{1}{4} g^4 \phi^2 T \int \frac{d^3 p}{(2\pi)^3} \frac{1}{(p^2 + m_{\text{eff}}^2)} T \sum_{k_0 \neq 0} \int \frac{d^3 k}{(2\pi)^3} \frac{1}{(K^2 + m^2)[(P+K)^2 + m^2]} \\
 &= \frac{1}{4} g^4 \phi^2 T \int \frac{d^3 p}{(2\pi)^3} \frac{1}{(p^2 + m_{\text{eff}}^2)} [O(\ln(T/\bar{\mu})) + O(p^2/T^2, m^2/T^2) + O(p^4/T^4, m^4/T^4) + \dots] \\
 &= \frac{1}{4} g^4 \phi^2 T [O(m \ln(T/\bar{\mu})) + O(m^3/T^2) + O(m^5/T^3) + \dots] \\
 &= O(g^5 T^4 \ln(T/\bar{\mu})) + O(g^7 T^4) + O(g^9 T^4) + \dots .
 \end{aligned} \tag{3.33}$$

Note that we have implicitly used dimensional regularization to make sense of UV divergent integrals such as $\int d^3 p p^n / (p^2 + m^2)$ and estimate their order as m^{n+1} .¹¹

We may compute heavy-loop diagrams, such as the first term in Fig. 10, by relating them to our results from unresummed perturbation theory. Figure 11 shows such a relation. None of the lines are resummed, and unlabeled lines represent the sum over *all* values of k_0 . The first term is the previous, unresummed result of (3.19), the second term is $O(g^5 T^4)$ as discussed above, and the last term is a two-loop diagram in three dimensions. Combining with Fig. 10, resummation of the setting-sun diagram is therefore implemented by Fig. 12. We now need the difference of two three-dimensional graphs, the

last two terms of Fig. 12, which differ only by the mass used in the propagators. One may either compute the three-dimensional integrals directly or note that the mass dependence in the four-dimensional result (3.19) can only come from the $k_0=0$ term at this order. So the three-dimensional graphs are each

$$\frac{1}{48(4\pi)^2} g^4 \phi^2 T^2 \left[\text{const} + 2 \ln \left[\frac{T^2}{m^2} \right] \right], \tag{3.34}$$

with m replaced by m_{eff} in the third term of Fig. 12. The total effect of the sum of terms in Fig. 12 is therefore to simply replace m by m_{eff} in the unresummed, four-dimensional result (3.19):

$$\mu^{2\epsilon} \mathcal{V}^{(b)} = \frac{1}{48(4\pi)^2} g^4 \mu^{2\epsilon} \phi^2 T^2 \left[\frac{1}{\epsilon} + \iota_\epsilon - \ln \left[\frac{\bar{\mu}^2}{T^2} \right] + 2 \ln \left[\frac{T^2}{m_{\text{eff}}^2} \right] + 2 - c_H \right] + O(g^5 T^4). \tag{3.35}$$

The resummation of the figure-eight diagram is shown in Fig. 13. The result is easily evaluated by referring to the review (3.32) of the expansion of $I(m)$. The three-dimensional piece of $I(m)$ is the mT term,

$$I_3(m) = -\frac{1}{4\pi} mT, \tag{3.36}$$

and the contribution due to heavy modes is everything else:

$$\begin{aligned}
 I_h(m) &= \frac{1}{12} T^2 (1 + \epsilon \iota_\epsilon) - \frac{1}{64\pi^2} m^2 \left[\frac{1}{\epsilon} + \ln \left[\frac{\bar{\mu}^2}{T^2} \right] - 2c_B \right] \\
 &+ O(m^4/T^2) + O(\epsilon m^2).
 \end{aligned} \tag{3.37}$$

The resummation of the figure eight is then

$$\begin{aligned}
 \mu^{2\epsilon} \mathcal{V}^{(a)} &= \text{const} - \frac{1}{48 \times 4\pi} g^2 m_{\text{eff}} T^3 + \frac{1}{8(4\pi)^2} g^2 m_{\text{eff}}^2 T^2 \\
 &- \frac{1}{48(4\pi)^2} g^2 m^2 T^2 \left[\frac{1}{\epsilon} + \iota_\epsilon + \ln \left[\frac{\bar{\mu}^2}{T^2} \right] - 2c_B \right] \\
 &+ O(g^5 T^4).
 \end{aligned} \tag{3.38}$$

Note that this is not simply the substitution of $m \rightarrow m_{\text{eff}}$ into the unresummed result.

Resummation of the counterterm diagrams of Figs.

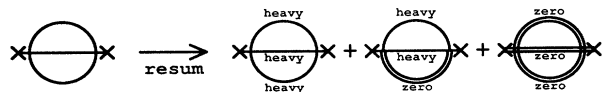


FIG. 10. Resummation of Fig. 7(b). Double lines are resummed, “heavy” denotes $k_0 \neq 0$ modes and “zero” denotes $k_0 = 0$ modes.

¹¹The reader may be concerned by this. It is possible, but cumbersome, to reorganize the three-dimensional ($k_0=0$) integrals that we shall encounter in implementing resummation at two loops so that they are UV convergent. For instance, the difference between the resummed and unresummed results takes the form $\int d^3 p p^n [(p^2 + m_{\text{eff}}^2)^{-1} - (p^2 + m^2)^{-1}]$, which is more UV convergent. Also, we are only interested in the ϕ dependence of the potential, and so may instead evaluate $d/d\phi$ of the potential, which makes the UV behavior even more convergent. With enough care, one may draw the same conclusions about which terms are negligible from UV convergent integrals.

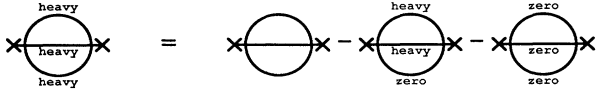


FIG. 11. Relation between a heavy contribution and the un-resummed graph.

7(c) and 7(d) do not change the unresummed results (3.20) and (3.21) through $O(g^4 T^4)$. The thermal counterterm of Fig. 8 now only applies to the $k_0=0$ modes, giving

$$\mu^{2\epsilon} \mathcal{V}^{(CT)} = \frac{1}{48 \times 4\pi} g^2 m_{\text{eff}} T^3. \quad (3.39)$$

For the one-loop result of (3.6) and (3.7), resummation affects only the $m^3 T$ term arising from the $k_0=0$ modes:

$$\mu^{2\epsilon} \mathcal{V}^{(1)}(\phi) = \mu^{2\epsilon} V_{\text{bare}}(\phi) + J_R[m(\phi)], \quad (3.40)$$

$$J_R(m) = \text{const} + \frac{1}{24} m^2 T^2 - \frac{1}{12\pi} m^3_{\text{eff}} T - \frac{1}{64\pi^2} m^4 \left[\frac{1}{\epsilon} + \ln \left[\frac{\bar{\mu}^2}{T^2} \right] - 2c_B \right] + O(m^6/T^2). \quad (3.41)$$

The sum of all these contributions reproduces the previous resummed, two-loop result (3.29), giving an explicit example that the exact details of the resummation prescription are unimportant.

IV. THE ABELIAN HIGGS MODEL

We now turn to the simplest example of a spontaneously broken gauge theory: the Abelian Higgs model, defined by the Lagrangian

$$\mathcal{L} = -\frac{1}{4} F^2 + |D\Phi|^2 - V(|\Phi|^2), \quad (4.1)$$

$$V(|\Phi|^2) = -v^2 |\Phi|^2 + \frac{1}{3!} \lambda |\Phi|^4,$$

where Φ is a complex field and $D_\mu \Phi = (\partial_\mu - ie A_\mu) \Phi$. We shall typically express the potential in terms of $\phi = \sqrt{2} \Phi$ so that it takes the canonical form (2.1). We now return to the original power-counting rules of Table I and assume $\lambda \sim e^3$.

Now consider the masses of particles in a background field ϕ . In most gauges, such a background field induces mixing between the scalar and the unphysical (k_μ) polarization of the vector, as shown in Fig. 14. When studying effective potentials $V(\phi)$, mixing arises even in (consistently defined) R_ξ gauges because there is no single, ϕ -independent gauge-fixing condition that will eliminate

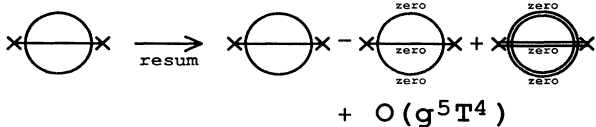


FIG. 12. Rewriting of Fig. 10.

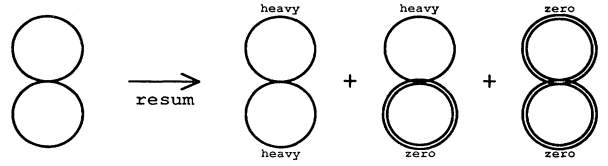


FIG. 13. Resummation of Fig. 7(a).

mixing for all values of the background field ϕ [17,25]. However, there exists a gauge choice, the Landau gauge, where the mixing effectively vanishes, because in this gauge the unphysical vector polarization does not propagate. In order to avoid having to diagonalize propagators, which increases the number and complexity of Feynman diagrams, we shall restrict ourselves to Landau gauge. Our gauge-fixing condition is therefore

$$\mathcal{L}_{\text{GF}} = -\frac{1}{2\xi} (\partial \cdot A)^2 - \bar{\eta} \partial^2 \eta, \quad \xi \rightarrow 0, \quad (4.2)$$

where the ghost η is completely decoupled in this Abelian model. The Euclidean vector propagator in Landau gauge is

$$G_{\mu\nu}(K) = \frac{\delta_{\mu\nu} - K_\mu K_\nu / K^2}{K^2 + M^2}. \quad (4.3)$$

In the best of worlds it would be nice to compute results in a variety of gauges and check that physical quantities are indeed gauge invariant, but we have not had the perseverance to do so.

In Landau gauge, the masses of fluctuations in the background ϕ are classically

$$\begin{aligned} M^2(\phi) &= e^2 \phi^2 \quad (\text{vector}), \\ m_1^2(\phi) &= -v^2 + \frac{1}{2} \lambda \phi^2 \quad (\text{physical Higgs boson}), \\ m_2^2(\phi) &= -v^2 + \frac{1}{6} \lambda \phi^2 \quad (\text{unphysical Goldstone boson}). \end{aligned} \quad (4.4)$$

We can now easily construct the (unresummed) one-loop potential:

$$\begin{aligned} \mu^{2\epsilon} \mathcal{V}_R^{(1)} &= \mu^{2\epsilon} V_{\text{bare}}(\phi) + (3 - 2\epsilon) J[M(\phi)] \\ &\quad + J[m_1(\phi)] + J[m_2(\phi)] + \text{const} \end{aligned} \quad (4.5)$$

(where the extra constant arises from the decoupled ghost contribution). As before, the singularities in the expansion (3.7) of $J(m)$ cancel against those in the bare potential V_{bare} . The explicit counterterms are given in Appendix A.

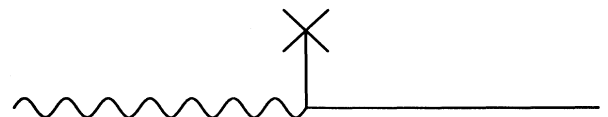


FIG. 14. Mixing between the k_μ polarization of A_μ and the unphysical Higgs boson in a background field ϕ .

A. Two-loop results without resummation

The two-loop diagrams are shown in Fig. 15, where we have ignored purely scalar diagrams since they are suppressed by $\lambda \sim e^3$ and are of lower order than $e^4 T^4$. Ignoring resummation for now, we shall discuss how to compute the diagrams. Figure 15(a) contributes

$$\mu^{2\epsilon} V_{\mathbf{K}}^{(a)} = -\frac{1}{2} e^2 \mu^{4\epsilon} \int_P \int_Q \frac{4Q^2 - 4(P \cdot Q)^2 / P^2}{(P^2 + M^2)(Q^2 + m_1^2)[(P+Q)^2 + m_2^2]} . \quad (4.6)$$

This may be rewritten in terms of integrals similar to $I(m)$ and $H(m)$ of the last section by repeatedly expanding factors in the numerator as sums of denominators, e.g.,

$$2(P \cdot Q) = [(P+Q)^2 + m_2^2] - (P^2 + M^2) - (Q^2 + m_1^2) + (M^2 + m_1^2 - m_2^2) , \quad (4.7)$$

and by noting that

$$\frac{1}{P^2(P^2 + M^2)} = \frac{1}{M^2 P^2} - \frac{1}{M^2(P^2 + M^2)} . \quad (4.8)$$

In this way, (4.6) may be rewritten as

$$\mu^{2\epsilon} V_{\mathbf{K}}^{(a)} = -\frac{1}{2} e^2 \left\{ I(M)[I(m_1) + I(m_2)] - I(m_1)I(m_2) + (M^2 - 2m_1^2 - 2m_2^2)\bar{H}(m_1, m_2, M) \right. \\ \left. + \frac{m_1^2 - m_2^2}{M^2} [I(M) - I(0)][I(m_1) - I(m_2)] + \frac{(m_1^2 - m_2^2)^2}{M^2} [\bar{H}(m_1, m_2, M) - \bar{H}(m_1, m_2, 0)] \right\} , \quad (4.9)$$

where $I(m)$ is (3.11) as before and

$$\bar{H}(m_1, m_2, m_3) = \mu^{4\epsilon} \int_P \int_Q \frac{1}{(P^2 + m_1^2)(Q^2 + m_2^2)[(P+Q)^2 + m_3^2]} . \quad (4.10)$$

\bar{H} is simply a generalization of the $H(m)$ of the last section to the case of unequal masses.

We now need a high-temperature expansion of \bar{H} . It is easy to relate \bar{H} to $H(m)$ by considering the difference

$$\bar{H}(m_1, m_2, m_3) - H(m) = \mu^{4\epsilon} \int_P \int_Q \left\{ \frac{1}{(P^2 + m_1^2)(Q^2 + m_2^2)[(P+Q)^2 + m_3^2]} \right. \\ \left. - \frac{1}{(P^2 + m^2)(Q^2 + m^2)[(P+Q)^2 + m^2]} \right\} \quad (4.11)$$

for any choice of masses small compared to T . The difference is more UV convergent than either alone, and the contributions to the difference involving heavy ($p_0 \neq 0$ or $q_0 \neq 0$) modes are suppressed by the small masses. The dominant contribution to the difference comes from the three-dimensional piece ($p_0 = q_0 = 0$) and is of order T^2 . The simplest way to evaluate it is to switch to configuration space,¹² and set ϵ to zero since the difference (4.11) is UV convergent in three dimensions. The three-dimensional propagator is simply $e^{-mr}/4\pi r$, and we obtain

$$\bar{H}(m_1, m_2, m_3) - H(m) = \frac{T^2}{(4\pi)^2} \int_0^\infty \frac{dr}{r} \{ \exp[-(m_1 + m_2 + m_3)r] - \exp(-3mr) \} + \mathcal{O}(m^2) \\ = \frac{T^2}{(4\pi)^2} \{ -\ln(m_1 + m_2 + m_3) + \ln(3m) \} + \mathcal{O}(m^2) . \quad (4.12)$$

Adding this to the result (3.17) for $H(m)$ gives

$$\bar{H}(m_1, m_2, m_3) = H \left[\frac{m_1 + m_2 + m_3}{3} \right] \\ = \frac{1}{64\pi^2} T^2 \left[\frac{1}{\epsilon} + \iota_\epsilon + \ln \left[\frac{\bar{\mu}^2}{T^2} \right] + 4 \ln \left[\frac{3T}{m_1 + m_2 + m_3} \right] + 2 - c_H \right] + \mathcal{O}(m^2) + \mathcal{O}(\epsilon T^2) . \quad (4.13)$$

(4.9) may now easily be expanded:

¹²We thank Lowell Brown for this observation.

$$\mu^{2\epsilon} \mathcal{V}_R^{(a)} = \frac{e^2 M T^3}{12(4\pi)} - \frac{e^2 M^2 T^2}{24(4\pi)^2} \left[\frac{1}{\epsilon} + \nu_\epsilon + \ln \left[\frac{\bar{\mu}^2}{T^2} \right] + 12 \ln \left[\frac{3T}{M} \right] + 6 + 4c_B - 3c_H \right] + \mathcal{O}(e^{9/2} T^4). \quad (4.14)$$

The $\mathcal{O}(e^{9/2} T^4)$ comes from terms of order $e^2 m M T$. Though one could keep track of such terms in a two-loop calculation, and so improve the error to $\mathcal{O}(e^5 T^4)$, we have not bothered to do so. We shall focus only on the *leading* correction to the one-loop potential for $e^4 \ll \lambda \ll e^2$.

The other graphs may be computed in similar fashion, and the results are given in Appendix A.

B. Resummation: Effective masses

We need to resum the propagators to include the dominant thermal corrections to the masses. We shall use the prescription of Sec. III D (method II) of only resumming the static $k_0=0$ modes. In the Abelian Higgs model, the longitudinal (A_0) mass at ($p_0=0, \mathbf{p} \rightarrow 0$) becomes

$$M_L^2 = e^2 \phi^2 + \frac{1}{3} e^2 T^2 \quad (4.15)$$

while the transverse mass remains the same, which we shall continue to denote by M :

$$M^2 = e^2 \phi^2. \quad (4.16)$$

The leading contribution to the scalar thermal mass changes the m_i^2 of (4.4) to

$$\bar{m}_i^2(\phi) = m_i^2(\phi) + \left[\frac{1}{2} \lambda + \frac{1}{6} \lambda + 3e^2 \right] \frac{T^2}{12}. \quad (4.17)$$

The resummation of the one-loop potential (4.5) gives

$$\begin{aligned} \mathcal{V}^{(1)} = & \frac{1}{2} \left[-v^2 + \left[\frac{2}{3} \lambda + 3e^2 \right] \frac{T^2}{12} \right] \phi^2 \\ & - \frac{1}{12\pi} (2M^3 + M_L^3) T + \frac{1}{4!} \lambda \phi^4 \\ & - \frac{3M^4}{64\pi^2} \left[\ln \left[\frac{\bar{\mu}^2}{T^2} \right] - \frac{2}{3} - 2c_B \right] + \mathcal{O}(e^{9/2} T^4). \end{aligned} \quad (4.18)$$

We can now proceed as we did in Sec. III. Before doing so, we should dwell a little more on the convergence

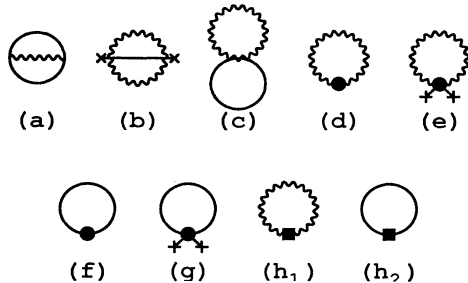


FIG. 15. Two-loop diagrams in the Abelian Higgs model.

of the loop expansion. [The following discussion is important for providing a well-behaved loop expansion but will turn out to have little practical importance for the actual computation of the two-loop potential to $\mathcal{O}(e^4 T^4)$.] Consider the multiloop diagram of Fig. 16. The cost of adding loop A to the diagram is $e^4 \phi^2 T / M^3$; the $e^4 \phi^2$ comes from the vertices, the T because it is a one-loop integral that is not quadratically divergent, and the $1/M^3$ to make a dimensionless quantity. More specifically, the $1/M^3$ arises because adding the loop added three propagators to the diagram (two vector and one scalar) and a loop integral $d^3 k$ which is dominated by its infrared behavior. Both the new loop A and the loop it is attached to are dominated by momenta of order M rather than m , and so each propagator gives $1/M^2$ and the new $d^3 k$ gives M^3 . The total loop cost of $e^4 \phi^2 T / M^3$ is the same order as $e^2 T / M \sim e$ (see Table I), which is the vector loop expansion parameter that we identified in the Introduction.

Ignoring the dominant $e^2 T^2$ piece that is absorbed by resummation, the cost of loop B is $e^2 T m / M^2 \sim e^{3/2}$ since the loops are dominated by momenta of order m for the scalar and M for the vector. Similarly, loop C cost $\lambda T / m \sim e^{3/2}$ after the dominant λT^2 piece is absorbed by resummation. Adding line D cost $e^2 T / M \sim e$. Adding line E , however, cost $e^2 T M / m^2 \sim 1$. So it would seem that the loop expansion parameter is not order e but instead order 1. The problem arises because of the difference of scales between m and M . When we defined the effective scalar masses \bar{m} in (4.17), we only included the dominant $\mathcal{O}(e^2 T^2)$ or $\mathcal{O}(\lambda T^2)$ contributions of vector or scalar loops to the self-energy. However, the subleading $\mathcal{O}(e^2 M T)$ vector-loop contribution is the same size as \bar{m}^2 itself since $\bar{m}^2 \sim e^3 T^2$; it is not a perturbation and so

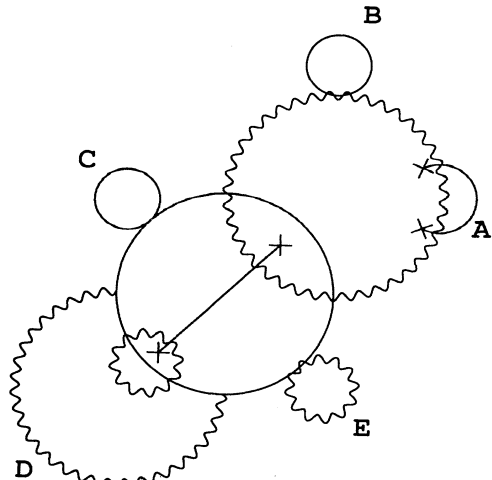


FIG. 16. A generic multiloop diagram.

must also be included in the resummation. (Yet higher-order terms *are* perturbations and so do not need to be included.) The new procedure for resummation may be viewed as follows: first integrate out all of the heavy modes to obtain an effective theory for momenta $k_0=0$ and $k \ll T$; next integrate out the vectors (and scalars with $k \sim M$) to obtain an effective theory for momenta $k_0=0$ and $k \ll M$; and only then finally integrate out scalar loops controlled by $k \sim \bar{m} \ll M$. This procedure is equivalent to modifying our resummation prescription by including the $O(e^2MT)$ corrections to the one-loop scalar mass (4.17):

$$\begin{aligned} \bar{m}_i^2(\phi) \rightarrow m_i^2(\phi) + \left[\frac{1}{2}\lambda + \frac{1}{6}\lambda + 3e^2 \right] \frac{T^2}{12} \\ - \frac{e^2}{4\pi} (2M + M_L)T - \frac{e^4\phi^2}{4\pi} \left[\frac{2}{M} + \frac{1}{M_L} \right] T. \end{aligned} \quad (4.19)$$

This result may be computed directly from one-loop diagrams or, more simply, from the second derivative through $O(e^3T^2)$ of the resummed one-loop potential (4.18). Using the resummation (4.19), the cost of adding a new loop will now always be $\lesssim e$.

Diagrammatically, this resummation corresponds to the dominant pieces of a subset of “once-iterated” ring diagrams, as shown in Fig. 17 for the improved scalar contribution to the one-loop potential.¹³ The smallest loops of the diagram are hard, with momenta of order T , the next smallest are vector loops with momenta of order $M \sim eT$, and the large Higgs loop is softer yet, with momenta of order $m \sim e^{3/2}T$. Because of the hierarchy of scales, it is a good approximation at each level of Fig. 18 to approximate resummed propagators $1/[p^2 + \Pi(p)]$ by $1/[p^2 + \Pi(0)]$.

Though the foregoing discussion was necessary to establish an adequate procedure for obtaining a controlled loop expansion, the details of resumming the scalar masses turn out not to be relevant at the order under consideration. Though the results of some graphs have potentially significant terms of the form e^2mT^3 , which would be affected by the details of how m is replaced by \bar{m} , all such terms cancel in the final potential. The m^2T^2 term of the one-loop potential is not modified to \bar{m}^2T^2 if we only resum $k_0=0$ modes (method II of Sec. III D). All other terms involving m are of lower order than $O(e^4T^4)$. [We would need to take care to use the correct resummation (4.19) for \bar{m} if we were keeping track of $O(e^{9/2}T^4)$ contributions to the potential.]

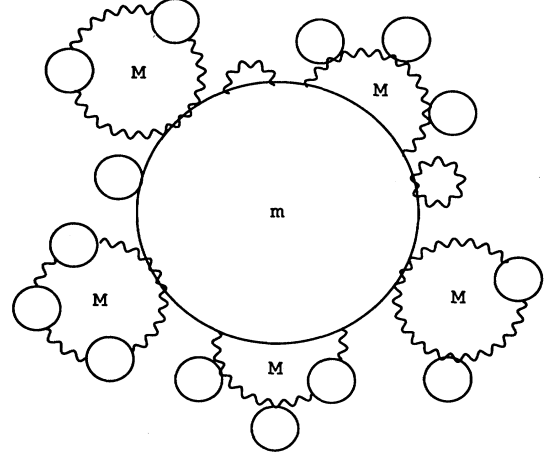


FIG. 17. Generic once-iterated ring diagram for the Higgs-loop contribution to the effective potential.

C. Resummation: Two-loop diagrams

Now let us turn to the resummation of actual diagrams. The resummation of Fig. 15(a) is depicted in Fig. 18.

In the last pair of terms of Fig. 18(b), resumming the vector line makes no difference because the A_0 polarization couples to the k_0 components of the scalar momenta, which are zero. The only difference between the last two diagrams is therefore the scalar masses. It is easy to see by examining the general result (4.9) for the setting-sun diagram, and remembering that the three-dimensional version (3.36) of $I(m)$ is simply $I_3(m) = -mT/4\pi$, that these three-dimensional diagrams do not depend on the scalar mass at $O(e^4T^4)$. So their difference is ignorable and may be dropped.

In the other two pairs of terms of Fig. 18(b), the heavy loops simply act as $O(e^2T^2)$ mass insertions in the light loops. For example, the first pair of terms contributes to the potential

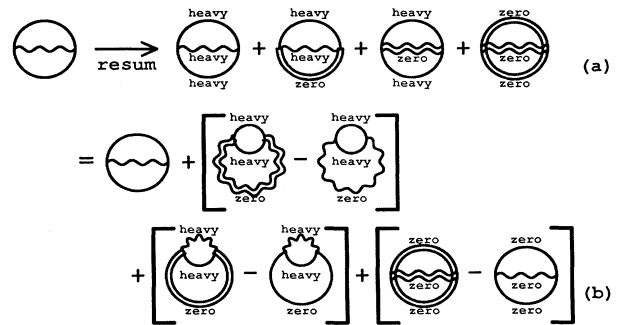


FIG. 18. Resummation of Fig. 15(a).

¹³The discussion of such diagrams appears in a related context in Ref. [26].

$$\begin{aligned}
& -\frac{1}{2}e^2T \int \frac{d^3p}{(2\pi)^3} \left[\frac{n_\mu n_\nu}{p^2+M_L^2} - \frac{n_\mu n_\nu}{p^2+M^2} \right] T \sum_{q_0 \neq 0} \int \frac{d^3q}{(2\pi)^3} \frac{(P+2Q)_\mu(P+2Q)_\nu}{(Q^2+m^2)[(P+Q)^2+m^2]} \\
& = -\frac{1}{2}e^2T \int \frac{d^3p}{(2\pi)^3} \left[\frac{n_\mu n_\nu}{p^2+M_L^2} - \frac{n_\mu n_\nu}{p^2+M^2} \right] T \sum_{q_0 \neq 0} \int \frac{d^3q}{(2\pi)^3} \frac{4Q_\mu Q_\nu}{Q^4} [1+O(p^2/Q^2, m^2/Q^2)+\dots] \\
& = -\frac{1}{4}T \int \frac{d^3p}{(2\pi)^3} \left[\frac{1}{p^2+M_L^2} - \frac{1}{p^2+M^2} \right] \frac{-1}{3}e^2T^2[1+O(p^2/T^2, m^2/T^2)+\dots] \\
& = -\frac{1}{12 \times 4\pi} e^2(M_L - M)T^3 + O(e^5T^4), \tag{4.20}
\end{aligned}$$

where $n_\mu=(1, \mathbf{0})$ and $P=(0, \mathbf{p})$. It is the MT^3 and mT^3 terms that resummation is supposed to eliminate. This does not occur on a graph-by-graph basis, but they cancel in the sum over graphs. The $M_L T^3$ and $\bar{m}T^3$ terms cancel against the counterterm graphs of Fig. 15(h). Evaluating the rest of Fig. 18(b) similarly, one finds

$$\mu^{2\epsilon}V^{(a)} = \mu^{2\epsilon}V_R^{(a)} - \frac{1}{12 \times 4\pi} e^2(M_L - M)T^3 + O(e^5T^4). \tag{4.21}$$

The results for the other diagrams may all be found in Appendix A. When added together, they give the full, improved two-loop potential:

$$\begin{aligned}
V^{(2)} = & \frac{1}{2}\phi^2(T) \left\{ -v^2(T) + \left[\frac{2}{3}\lambda(T) + 3e^2(T) \right] \frac{T^2}{12} - \frac{e^4T^2}{(4\pi)^2} \left[2 \ln \left[\frac{3T}{2M_L} \right] + 4 \ln \left[\frac{3T}{2M} \right] + \frac{29}{9} - \frac{2}{3}c_B - \frac{3}{2}c_H \right] \right\} \\
& - \frac{1}{12\pi} (2M^3 + M_L^3)T + \frac{1}{4!}\phi^4(T) \left[\lambda(T) + \frac{36e^4}{(4\pi)^2} \left[c_B + \frac{1}{3} \right] \right] + O(e^{9/2}T^4), \tag{4.22}
\end{aligned}$$

where

$$e^2(T) = e^2 + \frac{e^4}{3(4\pi)^2} \ln \frac{T^2}{\bar{\mu}^2} + O(e^5), \tag{4.23}$$

$$\lambda(T) = \lambda + \frac{18e^4}{(4\pi)^2} \ln \frac{T^2}{\bar{\mu}^2} + O(e^5), \tag{4.24}$$

$$\phi(T) = \phi \left[1 + \frac{3e^2}{2(4\pi)^2} \ln \frac{T^2}{\bar{\mu}^2} + O(e^3) \right], \tag{4.25}$$

$$v^2(T) = v^2 + O(e^5T^2). \tag{4.26}$$

It is important to remember that this result was derived in the high-temperature limit, and the $T \rightarrow 0$ limit of the terms shown in (4.22) is *not* the same as the zero-temperature potential. The $T \rightarrow 0$ limit of (4.22) is trivial since the $\lambda(T)\phi^4$ term vanishes if the scale of λ is run to zero. For the true potential at zero temperature, the relevant coupling is instead $\lambda(\phi)$. This distinction is important to keep in mind when using the two-loop result for numerical work.

D. The vacuum shift

How much do the two-loop corrections just computed affect the asymmetric vacuum at the phase transition? The simplest quantity to examine is the vacuum expectation value. This VEV is not a physical, gauge-invariant quantity [27], but the size of its shift due to two-loop corrections will still give us a good test of whether the loop corrections are small. In a companion work [28], one of us has instead computed the magnetic screening mass in the asymmetric vacuum, which is physical and

gauge invariant. (Actually, we suspect that the VEV may be gauge invariant to the order we have computed, but we do not know for sure.)

Normalize the potential so that $V(\phi, T)$ is zero at the origin. The VEV ϕ of the asymmetric vacuum at the critical temperature T is then determined by simultaneously solving

$$V(\phi, T) = 0, \quad \partial_\phi V(\phi, T) = 0. \tag{4.27}$$

Write $V = V_1 + \Delta V$ where V is the full potential, V_1 is some approximation (say, the one-loop potential), and ΔV is a small perturbation. Write $\phi = \phi_1 + \Delta\phi$ and $T = T_1 + \Delta T$ where ϕ_1 is the asymmetric vacuum of the approximation V_1 at its critical temperature T_1 ; that is,

$$V_1(\phi_1, T_1) = 0, \quad \partial_\phi V_1(\phi_1, T_1) = 0. \tag{4.28}$$

Linearizing the equations (4.27) in $\Delta\phi$ and ΔT , one finds

$$\Delta T \approx \frac{-\Delta V}{\partial_T V_1}, \tag{4.29}$$

$$\Delta\phi \approx \frac{\Delta V \partial_\phi \partial_T V_1 - (\partial_\phi \Delta V)(\partial_T V_1)}{(\partial_\phi^2 V_1)(\partial_T V_1)}, \tag{4.30}$$

where all the quantities are evaluated at the VEV. Note that $\Delta\phi/\phi$ is of order $\Delta V/V$, where V is the typical size of terms in the potential, and so $\Delta\phi/\phi$ is of order the loop expansion parameter.

Now identify V_1 with the one-loop potential and note that

$$\partial_T V_1 = \frac{1}{4}e^2T\phi^2 + O(e^3T^2). \tag{4.31}$$

Plugging into the solution (4.30) for $\Delta\phi$,

$$\frac{\Delta\phi}{\phi} = -\frac{\phi}{\bar{m}_1^2} \partial_\phi \left[\frac{\Delta V}{\phi^2} \right] + \mathcal{O}(e^{3/2}). \quad (4.32)$$

It is important when applying this formula to remember that $\Delta V(\phi, T)$ should be replaced by $\Delta V(\phi, T) - \Delta V(0, T)$ if the potential is not already normalized to zero at $\phi=0$. This result has the important property that it *vanishes* at leading order if ΔV is proportional to ϕ^2 . So the only *two-loop* contributions to the potential (4.22) which contribute to the (leading-order) shift in the VEV are those that involve logarithms of masses: the $e^4 T^2 \phi^2 \ln M(\phi)$ and $e^4 T^2 \phi^2 \ln M_L(\phi)$ terms. (The $e^4 \phi^4$ terms, which would also contribute if taken as part of ΔV , came from the *one-loop* contributions.) Equation (4.32) applies to all the models we shall examine.

For the Abelian Higgs model, (4.32) reduces to

$$\frac{\Delta\phi}{\phi} \approx \frac{e^4 T^2}{(4\pi)^2 \bar{m}_1^2} \left[2 + \frac{M^2}{M_L^2} \right], \quad (4.33)$$

where M_L , M , and \bar{m}_1 are as usual the effective masses at the phase transition given by (4.15), (4.16), and (4.19), and where the one-loop approximation to the VEV ϕ is sufficient for the right-hand side above. The one-loop approximation to ϕ does not have a simple form in terms of T , $M_W(T=0)$, and $m_H(T=0)$ (at least not for the whole range $e^4 \ll \lambda \ll e^2$), and is best computed numerically.

V. FERMIONS

Fermions are simpler to deal with than bosons because they do not require resummation. This is because Euclidean fermions have frequencies $k_0 = (2n+1)\pi T$ which are never zero, and so their self-energies may always be treated perturbatively. For the same reason, the two-loop contributions to the potential that involve fermions will never have a logarithmic dependence on the fermion mass $m_f(\phi)$ and so will not affect the shift in the VEV. Two-loop fermionic diagrams do contribute to the effective potential at $\mathcal{O}(g^4 T^4)$, however, and so we shall treat them here (and later in our discussion of the minimal standard model) for completeness.

As a simple example of a theory analogous to the weak interactions, let us chirally couple a single Dirac fermion to the Abelian Higgs model:

$$\begin{aligned} \mathcal{L} &\rightarrow \mathcal{L} + \bar{\psi} \left[\not{\partial} - ie \mathbf{A} \left(\frac{1-\gamma_5}{2} \right) \right] \psi \\ &+ g_Y \bar{\psi} \left[\Phi^* \left(\frac{1-\gamma_5}{2} \right) + \Phi \left(\frac{1+\gamma_5}{2} \right) \right] \psi \\ &= \mathcal{L} + \bar{\psi} \left[\not{\partial} - ie \mathbf{A} \left(\frac{1-\gamma_5}{2} \right) \right] \psi + \frac{g_Y}{\sqrt{2}} \bar{\psi} (\phi_1 + i\gamma_5 \phi_2) \psi. \end{aligned} \quad (5.1)$$

$$\text{tr}(\gamma_5 \gamma_\mu \gamma_\nu \gamma_\sigma \gamma_\tau) \text{ is antisymmetric,} \quad (5.8)$$

$$\text{tr}(\gamma_5 \gamma_\mu \gamma_\nu \gamma_\sigma \gamma_\tau) = 4i \epsilon_{\mu\nu\sigma\tau} + \mathcal{O}(\epsilon) \times \text{ambiguity, on the four-dimensional subspace } \mu, \nu, \sigma, \tau = 0, 1, 2, 3. \quad (5.9)$$

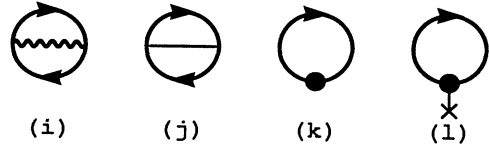


FIG. 19. Two-loop diagrams involving fermions.

We shall treat the Yukawa coupling g_Y as being of the same order as the gauge coupling e . The fermion mass in the presence of a background field ϕ is

$$m_f = \frac{1}{\sqrt{2}} g_Y \phi, \quad (5.2)$$

and the one-loop potential now picks up the familiar fermionic contribution

$$\mu^{2\epsilon} V^{(1)} \rightarrow \mu^{2\epsilon} V^{(1)} + 4J_f(m_f), \quad (5.3)$$

where [17]

$$\begin{aligned} J_f(m_f) &= -\frac{1}{2} \mu^{2\epsilon} \int \frac{d^4 K}{K} \ln(K^2 + m_f^2) \\ &= \text{const} + \frac{1}{48} m_f^2 T^2 \\ &+ \frac{1}{64\pi^2} m_f^4 \left[\frac{1}{\epsilon} + \ln \left(\frac{\bar{\mu}^2}{T^2} \right) - 2c_F \right] \\ &+ \mathcal{O}(m^6/T^2) + \mathcal{O}(\epsilon), \end{aligned} \quad (5.4)$$

and where we have defined the constant

$$c_F = \ln \pi - \gamma_E = c_B - 2 \ln 2. \quad (5.5)$$

The superscript (f) on the integral indicates that the frequency sums are over fermionic momenta $k_0 = (2n+1)\pi T$. The factor of 4 in (5.3) corresponds to the four components of a Dirac fermion. As is conventional in $\overline{\text{MS}}$ regularization, we take the Dirac trace of one to be $\text{tr} \mathbb{1} = 4$ rather than $2^{2-\epsilon}$.

Our working definition of γ_5 in dimensional regularization is the naive one that [29]

$$\{\gamma_5, \gamma_\mu\} = 0, \quad (5.6)$$

$$\gamma_5^2 = 1. \quad (5.7)$$

This definition is adequate for calculations that do not require traces involving an odd number of γ_5 's. Additional properties are

The anomaly is intimately related to the fact that the ambiguous term above cannot be explicitly defined. In our calculation, however, this term will never be relevant.

The new two-loop diagrams are shown in Fig. 19. As an example, take Fig. 19(i) and expand numerators in terms of denominators as we did in (4.6)–(4.9) for the Abelian Higgs model:

$$\begin{aligned} \mu^{2\epsilon} V_R^{(i)} &= -\frac{1}{2} e^2 \mathfrak{F}_P^{(f)} \mathfrak{F}_Q^{(f)} \frac{\delta_{\mu\nu} - (P+Q)_\mu (P+Q)_\nu / (P+Q)^2}{(P^2+m_f^2)(Q^2+m_f^2)[(P+Q)^2+M^2]} \text{tr}(-i\not{P}+m_f)\gamma_\mu \left[\frac{1-\gamma_5}{2} \right] (i\not{Q}+m_f)\gamma_\nu \left[\frac{1-\gamma_5}{2} \right] \\ &= -\frac{1}{8} e^2 \mathfrak{F}_P^{(f)} \mathfrak{F}_Q^{(f)} \frac{\delta_{\mu\nu} - (P+Q)_\mu (P+Q)_\nu / (P+Q)^2}{(P^2+m_f^2)(Q^2+m_f^2)[(P+Q)^2+M^2]} \text{tr} \not{P} \gamma_\mu \not{Q} \gamma_\nu \\ &= e^2 \{ (1-\epsilon) [I_f(m_f)]^2 - 2(1-\epsilon) I_f(m_f) I(M) + [(1-2\epsilon)m_f^2 - (1-\epsilon)M^2] \bar{H}_{ff}(m_f, m_f; M) \}. \end{aligned} \quad (5.10)$$

I_f and \bar{H}_{ff} are defined analogously to the bosonic I and \bar{H} of previous sections:

$$I_f(m_f) = \mu^{2\epsilon} \mathfrak{F}_K^{(f)} \frac{1}{K^2+m_f^2}, \quad (5.11)$$

$$\bar{H}_{ff}(m_{f2}, m_{f1}; m) = \mu^{4\epsilon} \mathfrak{F}_K \mathfrak{F}_Q \frac{1}{(K^2+m_{f2}^2)(Q^2+m_{f1}^2)[(P+Q)^2+m^2]}. \quad (5.12)$$

The high-temperature expansion of $I_f(m_f)$ may be obtained from (5.4) using $I_f = -m_f^{-1} dJ/dm_f$:

$$I_f(m) = -\frac{1}{24} T^2 - \frac{1}{16\pi^2} m^2 \left[\frac{1}{\epsilon} + \ln \left[\frac{\bar{\mu}^2}{T^2} \right] - 2c_F \right] + O(m^4/T^2) - \epsilon \iota_\epsilon^{(f)} \frac{1}{24} T^2 + O(\epsilon m^2). \quad (5.13)$$

In our earlier calculations, it turned out that the coefficient ι_ϵ of the ϵT^2 term of $I(m)$ was unimportant because it canceled in the final answer. When fermions are added to the theory, one finds that the final result *does* depend on the combination $\iota_\epsilon^{(f)} - \iota_\epsilon$, which it behooves us to calculate. One may find by a derivation of I_f similar to that for I in (3.32) that

$$\iota_\epsilon^{(f)} = \iota_\epsilon - 2 \ln 2. \quad (5.14)$$

We shall always make this substitution for $\iota_\epsilon^{(f)}$, and in this way the ι_ϵ 's will cancel in the final answer for the effective potential.

The leading $O(T^2)$ contribution to \bar{H}_{ff} turns out to *vanish*, and

$$\bar{H}_{ff}(m_{f2}, m_{f1}; m) = O(mT) + O(\epsilon T^2). \quad (5.15)$$

A derivation is given in Appendix B. The consequence of (5.15) is that the \bar{H}_{ff} term in (5.10) may be ignored when studying the effective potential through $O(e^4 T^4)$. \bar{H}_{ff} terms are similarly ignorable in all of the diagrams we shall calculate.

The high-temperature expansion of our result (5.10) for Fig. 19(i) is then

$$\begin{aligned} \mu^{2\epsilon} V_R^{(i)} &= -\frac{e^2 M T^3}{12 \times 4\pi} + \frac{e^2 m_f^2 T^2}{4(4\pi)^2} \left[\frac{1}{\epsilon} + \iota_\epsilon + \ln \left[\frac{\bar{\mu}^2}{T^2} \right] - 1 - 2c_F - \frac{2}{3} \ln 2 \right] \\ &\quad - \frac{e^2 M^2 T^2}{12(4\pi)^2} \left[\frac{1}{\epsilon} + \iota_\epsilon + \ln \left[\frac{\bar{\mu}^2}{T^2} \right] - 1 - 2c_B - 2 \ln 2 \right] + O(e^5 T^4). \end{aligned} \quad (5.16)$$

The results for the rest of the diagrams, and the results of resumming the $k_0=0$ modes of bosonic propagators, are given in Appendix A. The final two-loop potential is then

$V^{(2)} = [\text{Abelian Higgs result of (4.22)}]$

$$\begin{aligned} &+ \frac{1}{2} \phi(T)^2 \left\{ \frac{1}{12} g_Y^2(T) T^2 + \frac{g_Y^4 T^2}{(4\pi)^2} \left[-\frac{1}{2} c_F - \frac{1}{3} \ln 2 \right] \right. \\ &\quad \left. + \frac{e^2 g_Y^2 T^2}{(4\pi)^2} \left[-\frac{1}{12} - \frac{1}{2} c_F - \frac{1}{6} \ln 2 \right] + \frac{e^4 T^2}{(4\pi)^2} \left[\frac{1}{18} + \frac{1}{3} c_B + \frac{1}{3} \ln 2 \right] \right\} + \frac{1}{4!} \phi^4 \left[-\frac{12 c_F g_Y^4}{(4\pi)^2} \right], \end{aligned} \quad (5.17)$$

where the running couplings $\lambda(T)$ and so forth in (4.22) now include fermionic effects. (See Appendix A for formulas for the running couplings.)

VI. NON-ABELIAN THEORIES

Extending our analysis to non-Abelian theories is fairly straightforward; it merely involves the computation of some new graphs, shown in Fig. 20. In Appendix A, we give results for the SU(2) Higgs model with a single Higgs doublet, defined by

$$\mathcal{L} = -\frac{1}{4}F_{\mu\nu}^a F^{a\mu\nu} + |D\Phi|^2 - V(|\Phi|^2), \quad (6.1)$$

$$V(|\Phi|^2) = -v^2|\Phi|^2 + \frac{1}{3!}\lambda|\Phi|^4,$$

where Φ is an SU(2) doublet and

$$D_\mu\Phi = (\partial_\mu - i\frac{1}{2}gA_\mu \cdot \tau)\Phi. \quad (6.2)$$

We once again normalize ϕ to $\phi^2 = 2|\Phi|^2$.

Reducing the graphs of Fig. 20 to simple scalar integrals such as $I(m)$ and $\bar{H}(m_1, m_2, m_3)$ turns out to require the introduction of a new function:

$$L(m_1, m_2) = \int \frac{d^4P}{(2\pi)^4} \int \frac{d^4Q}{(2\pi)^4} \frac{(P \cdot Q)^2}{P^2(P^2 + m_1^2)Q^2(Q^2 + m_2^2)}. \quad (6.3)$$

One can derive a high-temperature expansion of this function, which we give in Appendix B, but it is unnecessary

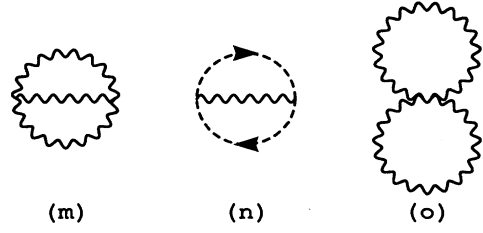


FIG. 20. Additional graphs needed for a non-Abelian theory.

because terms involving $L(m_1, m_2)$ cancel exactly between Figs. 20(m) and 20(o).

The only part of the calculation of the two-loop potential that is not a completely straightforward extension of our previous model calculations is the resummation of Fig. 20(m). The resummation is shown in Fig. 21. Recall that only the longitudinal (A_0) polarization is resummed, and split propagators into longitudinal (L) and transverse (T) parts. By using the fact that the three-vector coupling vanishes for LLL and LTT when all frequencies p_0 are zero, Fig. 21 may be rewritten as Fig. 22. The three-dimensional diagram in the last pair of terms is easy to evaluate, and the result is given in Appendix A.

The total ring-improved two-loop potential is given by

$$V^{(2)} = \frac{1}{2}\phi^2(T) \left\{ -v^2(T) + \left[\lambda(T) + \frac{9}{4}g^2(T) \right] \frac{T^2}{12} + \frac{g^4 T^2}{(4\pi)^2} \left[\frac{107}{24} + \frac{5}{4}c_B - \frac{81}{64}c_H + \frac{9}{4} \ln \left[\frac{3T}{2M_L + M} \right] + \frac{63}{16} \ln \frac{T}{M} - \frac{3}{8} \ln \left[\frac{3T}{2M_L} \right] - \frac{3}{4} \ln \left[\frac{3T}{2M} \right] \right] \right\} + \frac{3g^2 T^2}{(4\pi)^2} \left[M_L M - 2M_{\text{Debye}}^2 \ln \left[\frac{2M_L + M}{2M_{\text{Debye}}} \right] \right] - \frac{T}{12\pi} (6M^3 + 3M_L^3) + \frac{1}{4!} \phi^4(T) \left[\lambda(T) + \frac{27g^4}{4(4\pi)^2} \left[c_B + \frac{1}{3} \right] \right], \quad (6.4)$$

where we have introduced the notation

$$M_{\text{Debye}}^2 = M_L^2 - M^2 \quad (6.5)$$

for the ϕ -independent thermal mass. Note that though the $M_L M$ term above is linear in ϕ as $\phi \rightarrow 0$, this linear term cancels against the $\phi \rightarrow 0$ behavior of the $M_{\text{Debye}}^2 \ln(2M_L + M)$ term.

We can now compute the relative shift in the VEV from its one-loop value using (4.32):

$$\frac{\Delta\phi}{\phi} \approx \frac{g^4 T^2}{(4\pi)^2 \bar{m}_1^2} \left[\frac{87}{32} + \frac{3M_{\text{Debye}}^2}{2M_L M} - \frac{3M^2}{16M_L^2} - \frac{3M_{\text{Debye}}^2}{M^2} \ln \left[\frac{2M_L + M}{2M_{\text{Debye}}} \right] \right], \quad (6.6)$$

where M , M_L , and \bar{m}_1 may be evaluated at the phase transition using the one-loop approximation. \bar{m}_1 is obtained by taking the second derivative of the one-loop potential through $\mathcal{O}(g^3 T^2)$:

$$\bar{m}_1^2 = m_1^2 + \left[\lambda + \frac{9}{4}g^2 \right] \frac{T^2}{12} - \frac{3g^2 M T}{4\pi} - \frac{3g^2 T}{16\pi} \left[\frac{M^2}{M_L} + M_L \right]. \quad (6.7)$$

Note that the $M_L M$ term in the potential contributes to

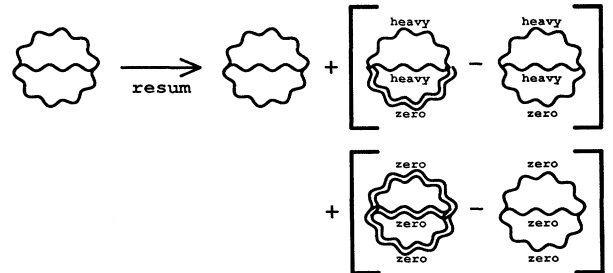


FIG. 21. Resummation of Fig. 20(m).

$\Delta\phi/\phi$, whereas only logarithms contributed in the Abelian case.

VII. THE MINIMAL STANDARD MODEL

Finally, consider the minimal standard model with a single Higgs doublet, which differs from the previous models only by the complexity of keeping track of the various couplings. Our conventions for coupling constants are such that

$$D_\mu = \partial_\mu + \frac{1}{2}g_2 A_\mu \cdot \tau + \frac{1}{2}Yg_1 B_\mu, \quad (7.1)$$

the hypercharge is normalized so that $Q = T_3 + Y/2$, and the Yukawa coupling is

$$g_Y \bar{q}_L \cdot \Phi t_R + \text{H.c.}, \quad (7.2)$$

where Φ is the full complex doublet. g_Y is the top quark coupling, which is the only Yukawa coupling that we treat as nonzero. We shall also include QCD interactions

$$M^2 = \begin{pmatrix} \frac{1}{4}g_2^2\phi^2 & -\frac{1}{4}g_1g_2\phi^2 \\ -\frac{1}{4}g_1g_2\phi^2 & \frac{1}{4}g_1^2\phi^2 \end{pmatrix} = \begin{pmatrix} \cos\theta_W & \sin\theta_W \\ -\sin\theta_W & \cos\theta_W \end{pmatrix} \begin{pmatrix} M_Z^2 \\ 0 \end{pmatrix} \begin{pmatrix} \cos\theta_W & -\sin\theta_W \\ \sin\theta_W & \cos\theta_W \end{pmatrix}. \quad (7.3)$$

When we include the Debye masses generated for the longitudinal (A_0) components at finite temperature however, one finds [20]

$$M_L^2 = \begin{pmatrix} \frac{1}{4}g_2^2\phi^2 + \left[\frac{5}{6} + \frac{n_f}{3}\right]g_2^2T^2 & -\frac{1}{4}g_1g_2\phi^2 \\ -\frac{1}{4}g_1g_2\phi^2 & \frac{1}{4}g_1^2\phi^2 + \left[\frac{1}{6} + \frac{5n_f}{9}\right]g_1^2T^2 \end{pmatrix} \\ \equiv \begin{pmatrix} \cos\tilde{\theta} & \sin\tilde{\theta} \\ -\sin\tilde{\theta} & \cos\tilde{\theta} \end{pmatrix} \begin{pmatrix} M_{LZ}^2 \\ M_{LY}^2 \end{pmatrix} \begin{pmatrix} \cos\tilde{\theta} & -\sin\tilde{\theta} \\ \sin\tilde{\theta} & \cos\tilde{\theta} \end{pmatrix}, \quad (7.4)$$

and we have diagonalized to define an effective mixing angle $\tilde{\theta}(\phi, T)$ and effective longitudinal masses $M_{LZ}(\phi, T)$ and $M_{LY}(\phi, T)$.

The result for the two-loop potential is given in Appendix A, where we list the contribution from each of the graphs of Fig. 23. Only those diagrams which give a ϕ -dependent contribution to the potential at $O(g^4T^4)$ are shown. Note that there is a QCD correction in Fig. 23(i₁) which gives a potentially large contribution to the potential of order $g_s^2g_Y^2\phi^2T^2$ but which, like all fermionic contributions, does not contribute to the leading-order shift in the VEV from its one-loop value.

It is cumbersome to write down the total answer for the two-loop potential, and we shall leave it in the form of Appendix A where each diagram is given separately. The reader should note that the relative shift in the VEV is given by (6.6) in the limit that $g_1 \rightarrow 0$. This is because, as discussed earlier, the fermion contributions do not affect the shift in the VEV except indirectly through their

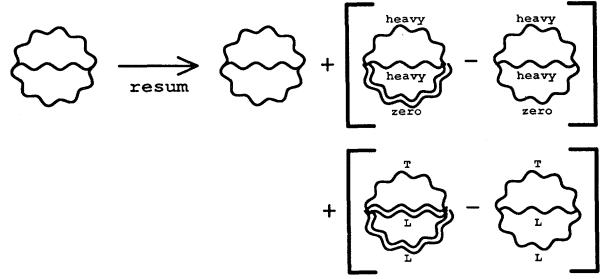


FIG. 22. Rewriting of Fig. 21. The L and T lines represent the longitudinal (A_0) and transverse polarizations of *only* the $p_0=0$ contributions.

for the quarks, with coupling g_s . The couplings g_1 , g_2 , g_Y , and g_s are formally treated as all having the same order of magnitude g . n_f represents the number of families and is 3 in the minimal standard model.

At zero temperature, the mass matrix for the Z boson and the photon, in the ($A^{(3)}, B$) basis, is

effect on the one-loop values of M , M_L , and \bar{m}_1 at the phase transition. For example, \bar{m}_1 in this limit changes from (6.7) to

$$\bar{m}_1^2 = m_1^2 + \left[\lambda + \frac{9}{4}g^2 + 3g_Y^2 \right] \frac{T^2}{12} - \frac{3g^2MT}{4\pi} \\ - \frac{3g^2T}{16\pi} \left[\frac{M^2}{M_L} + M_L \right]. \quad (7.5)$$

VIII. NUMERICAL RESULTS

As a test of the size of loop corrections, we shall now compute the shift $\Delta\phi$ in the VEV at the phase transition due to the inclusion of two-loop corrections in the minimal standard model. We do this numerically, by running couplings to $\bar{\mu}=T$ and then finding the phase transition for both the one-loop and two-loop approxima-

tions to the potential given in Appendix A.

As discussed in Sec. IV D, the relative size $\Delta\phi/\phi$ of this shift is $O(g)$, the loop expansion parameter. This means that we need to specify the original zero-temperature parameters of the theory, such as λ and g^2 , to relative order g in terms of physical quantities such as the zero-temperature Higgs-boson and vector masses.

Tree-level relations are adequate for most quantities, since corrections at zero temperature are suppressed by g^2 instead of g . The exceptions are λ and v^2 since they are $O(g^3)$ by our power-counting convention and receive $O(g^4)$ corrections at one loop. To obtain λ and v^2 in terms of physical masses, consider the one-loop potential at zero temperature:

$$V^{(1)}(\phi, T=0) = -\frac{1}{2}v^2\phi^2 + \frac{1}{4!}\lambda\phi^4 + \frac{6M_W^4(\phi)}{64\pi^2} \left[\ln \left[\frac{M_W^2(\phi)}{\bar{\mu}^2} \right] - \frac{5}{6} \right] \\ + \frac{3M_Z^4(\phi)}{64\pi^2} \left[\ln \left[\frac{M_Z^2(\phi)}{\bar{\mu}^2} \right] - \frac{5}{6} \right] - \frac{3m_t^4(\phi)}{16\pi^2} \left[\ln \left[\frac{m_t^2(\phi)}{\bar{\mu}^2} \right] - \frac{3}{2} \right] + O(m_1^4, m_2^4). \quad (8.1)$$

We shall refer to the zero-temperature VEV as σ . The physical Higgs-boson mass at the order under consideration is just the second derivative of this potential at σ .¹⁴ Solving for λ and v^2 in terms of the physical masses, one finds

$$\lambda = \frac{3\bar{m}_H^2}{\sigma^2} - \frac{3}{32\pi^2} \left\{ \frac{3}{2}g_2^4 \left[\ln \left[\frac{\bar{M}_W^2}{\bar{\mu}^2} \right] + \frac{2}{3} \right] + \frac{3}{4}(g_1^2 + g_2^2)^2 \left[\ln \left[\frac{\bar{M}_Z^2}{\bar{\mu}^2} \right] + \frac{2}{3} \right] - 12g_Y^4 \ln \left[\frac{\bar{m}_t^2}{\bar{\mu}^2} \right] \right\} + O(g^5), \quad (8.2)$$

$$v^2 = \frac{1}{2}\bar{m}_H^2 - \frac{\sigma^2}{64\pi^2} \left[\frac{3}{2}g_2^4 + \frac{3}{4}(g_1^2 + g_2^2)^2 - 12g_Y^4 \right] + O(g^2\bar{m}_H^2), \quad (8.3)$$

where the overbars denote that masses are evaluated at the VEV σ at zero temperature with renormalization scale $\bar{\mu}$, and where σ may be expressed as $\sigma = \bar{M}_W/g$.

Our numerical results for the shift $\Delta\phi/\phi$ due to two-loop corrections are shown in Fig. 24 as a function of m_H , assuming a top quark mass of 100 GeV. To get the solid line, we computed ϕ and T_c independently for both the one-loop potential and for our full result for the two-loop potential. To help control errors of the one-loop computation at very small m_H , we have used exact results for the one-loop fermion and vector contributions rather than high-temperature expansions.

Alternatively, the dashed line gives the simpler calculation of the pure SU(2) result (6.6) for the shift, which we have evaluated using the minimal standard model results for M_W and M_{LW} in place of M and M_L . We have also replaced \bar{m}_1^2 by the complete second derivative of the one-loop potential rather than by (7.5) because, due to fine cancellations among terms, the assumption that $g_1 \rightarrow 0$ used in (7.5) turns out to be a very bad approximation if the one-loop VEV and critical temperature were

¹⁴The physical Higgs-boson mass is actually determined by the pole of the Higgs propagator and so is given by the solution to the real-time dispersion relation $P^2 - M^2 = \Pi(P^2)$, where Π is the self-energy. The claim that it is given by the second derivative of the effective potential corresponds to the approximation $\Pi(P^2) \rightarrow \Pi(0)$ in this dispersion relation. The difference $\Pi(P^2) - \Pi(0)$ is order $g^5\sigma^2$ and does not affect our derivation of λ through $O(g^4)$.

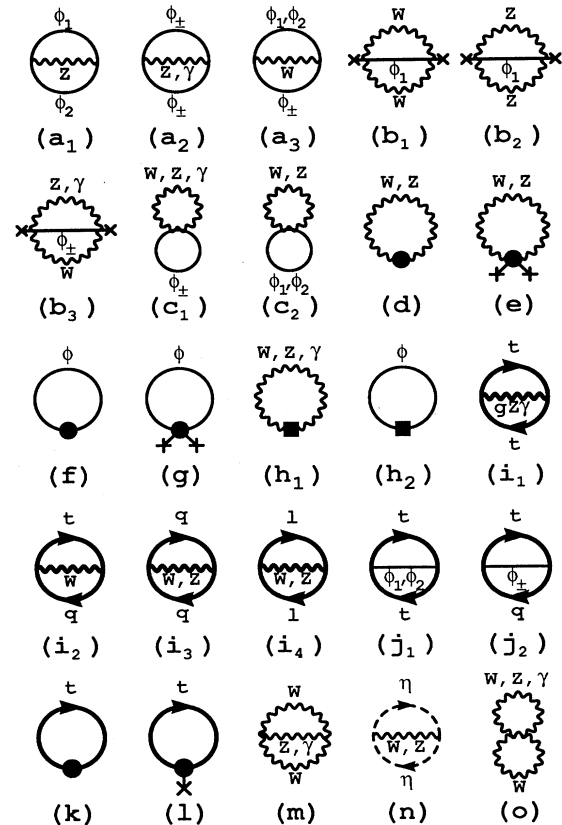


FIG. 23. Two-loop graphs for the minimal standard model. "q" indicates all quarks other than the top quark.

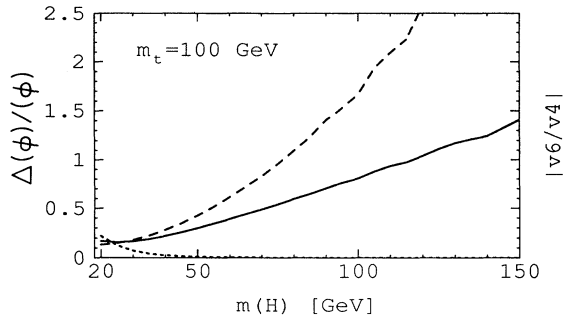


FIG. 24. Relative shift $\Delta\phi/\phi$ of the asymmetric vacuum at the critical temperature plotted vs the Higgs-boson mass. The solid line comes from using the full formula for the two-loop potential derived in this paper; the dashed line should approximately match it, up to yet high-order corrections in the loop expansion. The high-temperature expansion used in this paper is valid provided the dotted line (described in the text) is small compared to one.

computed with $g_1 \neq 0$. The dashed line should approximately match the solid line when both (i) $\Delta\phi/\phi$ is small and (ii) m_H is not so small that the high-temperature expansion has broken down. This correspondence is evident in Fig. 24. The deviation of the lines at large m_H is a manifestation of the breakdown of the loop expansion.

The dotted line in Fig. 24 is a diagnostic of our ubiquitous assumption ($\lambda \gg g^4$) that we may use the high-temperature expansion. It is the ratio of the $O(M^6/T^2)$ piece of the one-loop potential to the $O(M^4)$ piece. This ratio is taken in the asymmetric vacuum at the phase transition. More specifically,

$$v_4 = \frac{1}{32\pi^2} (6c_B M_W^4 + 3c_B M_Z^4 - 12c_F m_t^4), \quad (8.4)$$

$$v_6 = \frac{\xi(3)}{768\pi^4 T^2} (6M_W^6 + 3M_Z^6 - 7 \times 12m_t^6),$$

and the dotted line is $|v_6/v_4|$. One can see in Fig. 24 that the high-temperature expansion begins to break down at small m_h .

Figure 25 shows the result for ϕ/T at the phase transi-

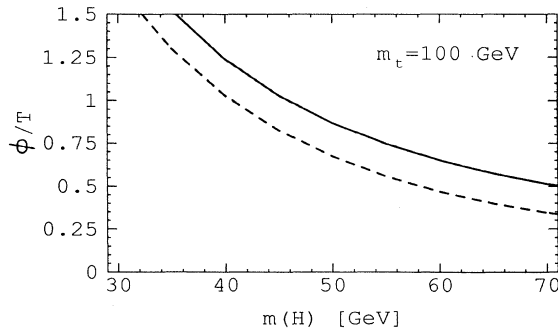


FIG. 25. The ratio ϕ/T at the phase transition. The dashed line is the one-loop result and the solid line is our two-loop result in Landau gauge.

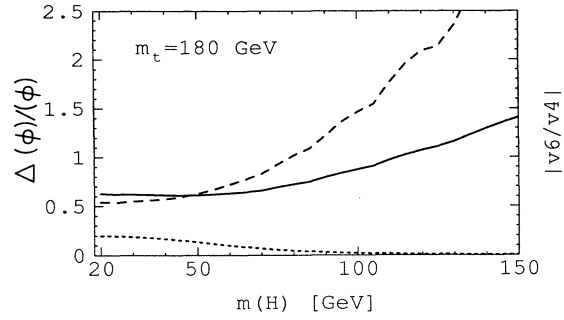


FIG. 26. Same as Fig. 24 but for $m_t = 180$ GeV.

tion, which is the quantity used in Ref. [12] to extract the upper bound on the Higgs-boson mass for weak baryogenesis. According to Ref. [12], a necessary requirement for a successful scenario of baryogenesis is that $\phi/T \geq 1$. The dashed and solid lines show our one-loop and two-loop results, respectively. At the experimental lower bound of 60 GeV, the one-loop result of 0.47 is inadequate. The two-loop corrections boost ϕ/T by 40% to roughly 0.65. This remains inadequate. Unfortunately, the corrections are large enough that this conclusion does not impress us as airtight—the validity of the loop expansion is only marginal here. Note that, for a consistent comparison at this order, the sphaleron mass and resulting limit on ϕ/T should also be consistently determined to the same order.

Figures 26 and 27 show our results for a top mass of 180 GeV. In parting, we remind the reader that the minimal standard model is only a specific testing ground for these issues and that the particular constraints just discussed are evaded in multiple-Higgs models.

Note added in proof. Shortly after completion of this work, related, independent work appeared by Bagnasco and Dine [31]. In the limit that $M \ll M_L$ (which is numerically a good approximation when deriving bounds for minimal standard model baryogenesis), these authors provide alternative and interesting methods for computing the most important two-loop corrections to the potential—the $\ln M$ terms and the strong interaction corrections. As discussed earlier, it is the $\ln M$ terms which are responsible for the two-loop correction to the VEV at the phase transition.

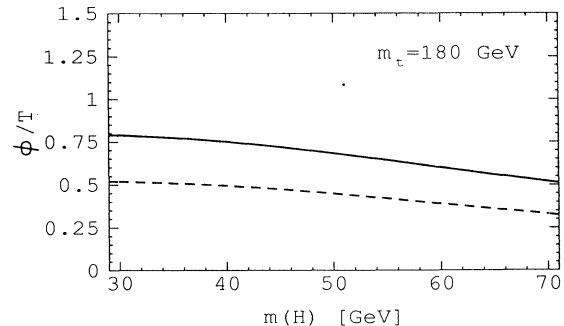


FIG. 27. Same as Fig. 25 but for $m_t = 180$ GeV.

ACKNOWLEDGMENTS

Both P.A. and O.E. were supported in part by the U.S. Department of Energy, Grant No. DE-FG06-91ER40614. P.A. was also supported in part by the Texas National Research Laboratory Commission. O.E. was also supported in part by the Fundación Andes Program No. C-12021/7. We are indebted to Larry Yaffe for many long and useful discussions and to Lowell Brown for the derivation of $\bar{H}(m_1, m_2, m_3)$ in three dimensions.

APPENDIX A: RESULTS FOR TWO-LOOP DIAGRAMS

In this appendix we collect two-loop results for individual diagrams in the various theories discussed in this paper. Since the theories involve many of the same diagrams, and differ only by group factors, we only compute them once. The \mathcal{D} functions defined at the end of this appendix are the results of diagrams where we have factored out a combination of coupling constants, symmetry factors, and group factors. The subscripts of the \mathcal{D} 's indicate the types of particles involved in the diagram: S for scalar, V for vector, f for fermion, and η for ghost. Note that the effective potential and the sum over diagrams have a relative minus sign in Euclidean space. We shall display only the ϕ -dependent pieces of contributions to the potential and shall not explicitly indicate the presence of temperature-dependent constants by "const." For brevity, we shall drop the unimportant $\mu^{2\epsilon}$ terms that

keep track of the dimensions of the potential V and the field ϕ ; but every instance of V and ϕ in this appendix should be understood as $\mu^{2\epsilon}V$ and $\mu^\epsilon\phi$. Throughout this appendix we adopt the notation

$$\frac{1}{\bar{\epsilon}} = \frac{1}{\epsilon}(1 + \epsilon\iota_\epsilon), \quad (\text{A1})$$

where ι_ϵ is the unimportant constant of (3.12), and we define

$$\bar{H}_3(m_1, m_2, m_3) = -\frac{1}{(4\pi)^2} T^2 \ln(m_1 + m_2 + m_3), \quad (\text{A2})$$

to be the (nonconstant) three-dimensional piece of \bar{H} , as in (4.12).

To actually use the formulas of this appendix for computing two-loop corrections numerically, sum the individual contributions but (1) drop all $1/\bar{\epsilon}$ terms, since they cancel; (2) set $\bar{\mu}$ to T and so drop all of the $\ln(\bar{\mu}^2/T^2)$ terms; and so (3) replace couplings g , masses ν , and fields ϕ everywhere by $g(T)$, $\nu(T)$, and $\phi(T)$.

Unresummed results for the diagrams in Secs. A 1 and A 2 may be obtained by replacing all \mathcal{D} 's by \mathcal{D}^R 's and dropping $V^{(h)}$.

1. Abelian Higgs model

Counterterms:

$$\begin{aligned} \phi_{\text{bare}} &= \left[1 + \frac{3e^2}{2(4\pi)^2\epsilon} + \dots \right] \phi, \quad A_{\text{bare}} = \left[1 - \frac{e^2}{6(4\pi)^2\epsilon} + \dots \right] A, \\ e_{\text{bare}}^2 &= \left[1 + \frac{e^2}{3(4\pi)^2\epsilon} + \dots \right] e^2 \mu^{2\epsilon}, \quad \lambda_{\text{bare}} = \left[\lambda + \frac{18e^4}{(4\pi)^2\epsilon} + \dots \right] \mu^{2\epsilon}, \\ \nu_{\text{bare}}^2 &= \left[1 - \frac{3e^2}{(4\pi)^2\epsilon} + \dots \right] \nu^2. \end{aligned} \quad (\text{A3})$$

Multiplicative corrections are shown only through order e^2 , and order λ corrections are left out since $\lambda \sim e^3$ by assumption. Running couplings and fields may be found by replacing $1/\epsilon \rightarrow \ln(T^2/\bar{\mu}^2)$ and $\phi_{\text{bare}} \rightarrow \phi(T)$, $e_{\text{bare}}^2 \rightarrow e^2(T)$, etc. above.

Masses:

$$M^2 = e^2\phi^2, \quad m_1^2 = -\nu^2 + \frac{1}{2}\lambda\phi^2, \quad m_2^2 = -\nu^2 + \frac{1}{6}\lambda\phi^2, \quad (\text{A4})$$

$$M_L^2 = e^2\phi^2 + \frac{1}{3}e^2T^2, \quad \tilde{m}_i^2 = m_i^2 + \left[\frac{2}{3}\lambda + 3e^2 \right] \frac{T^2}{12} + \dots \quad (\text{A5})$$

We shall not bother showing the subleading corrections to the thermal scalar mass, as in (4.19), since they cancel out in the final result for the potential to $O(e^4T^4)$.

One-loop result: See Eq. (4.18).

Two-loop diagrams of Fig. 15:

$$V^{(a)} = -\frac{1}{2}e^2\mathcal{D}_{SSV}(m_1, m_2, M), \quad (\text{A6a})$$

$$V^{(b)} = -\frac{1}{4}e^4\phi^2\mathcal{D}_{SVV}(m_1, M, M), \quad (\text{A6b})$$

$$V^{(c)} = -\frac{1}{4}e^2[\mathcal{D}_{SV}(m_1, M) + \mathcal{D}_{SV}(m_2, M)], \quad (\text{A6c})$$

$$V^{(d)} = \frac{e^2M^2T^2}{24(4\pi)^2} \left[\frac{1}{\bar{\epsilon}} - \frac{2}{3} \right] + O(e^5T^4), \quad (\text{A6d})$$

$$V^{(e)} = \frac{3e^4\phi^2T^2}{8(4\pi)^2} \left[\frac{1}{\bar{\epsilon}} - \frac{2}{3} \right] + O(e^5T^4), \quad (\text{A6e})$$

$$V^{(f)} = O(e^5T^4), \quad (\text{A6f})$$

$$\mathcal{V}^{(g)} = \frac{e^4 \phi^2 T^2}{2(4\pi)^2 \bar{\epsilon}} + \mathcal{O}(e^{11/2} T^4), \quad (\text{A6g})$$

$$\mathcal{V}^{(h)} = \frac{e^2 M_L T^3}{24\pi} + \frac{e^2 (\tilde{m}_1 + \tilde{m}_2) T^3}{32\pi} + \mathcal{O}(e^{9/2} T^4). \quad (\text{A6h})$$

2. Chiral Abelian Higgs model

Counterterms:

$$\begin{aligned} \phi_{\text{bare}} &= \left[1 + \frac{3e^2 - g_Y^2}{2(4\pi)^2 \epsilon} + \dots \right] \phi, \quad A_{\text{bare}} = \left[1 - \frac{e^2}{2(4\pi)^2 \epsilon} + \dots \right] A, \\ \psi_{L,\text{bare}} &= \left[1 - \frac{g_Y^2}{4(4\pi)^2 \epsilon} + \dots \right] \psi_L, \quad \psi_{R,\text{bare}} = \left[1 - \frac{g_Y^2}{4(4\pi)^2 \epsilon} + \dots \right] \psi_R, \\ e_{\text{bare}}^2 &= \left[1 + \frac{e^2}{(4\pi)^2 \epsilon} + \dots \right] e^2 \mu^{2\epsilon}, \quad \lambda_{\text{bare}} = \left[\lambda + \frac{18e^4 - 6g_Y^4}{(4\pi)^2 \epsilon} + \dots \right] \mu^{2\epsilon}, \\ \nu_{\text{bare}}^2 &= \left[1 - \frac{3e^2 - g_Y^2}{(4\pi)^2 \epsilon} + \dots \right] \nu^2, \quad g_{Y,\text{bare}} = \left[1 + \frac{2g_Y^2 - 3e^2}{2(4\pi)^2 \epsilon} + \dots \right] g_Y \mu^\epsilon. \end{aligned} \quad (\text{A7})$$

Formulas for running couplings may be obtained as in Sec. A 1.

Masses are as (A4) with

$$m_f^2 = \frac{1}{2} g_Y^2 \phi^2, \quad M_L^2 = e^2 \phi^2 + \frac{1}{2} e^2 T^2, \quad \tilde{m}_i^2 = m_i^2 + \left[\frac{2}{3} \lambda + 3e^2 + g_Y^2 \right] \frac{T^2}{12} + \dots \quad (\text{A8})$$

The one-loop result is

$$\begin{aligned} \mathcal{V}^{(1)} &= \frac{1}{2} \left[-\nu^2 + \left[\frac{2}{3} \lambda + 3e^2 + g_Y^2 \right] \frac{T^2}{12} \right] \phi^2 - \frac{1}{12\pi} (2M^3 + M_L^3) T + \frac{1}{4!} \lambda \phi^4 \\ &\quad - \frac{3M^4}{4(4\pi)^2} \left[\ln \left[\frac{\bar{\mu}^2}{T^2} \right] - \frac{2}{3} - 2c_B \right] + \frac{m_f^4}{(4\pi)^2} \left[\ln \left[\frac{\bar{\mu}^2}{T^2} \right] - 2c_F \right] + \mathcal{O}(e^{9/2} T^4). \end{aligned} \quad (\text{A9})$$

The two-loop diagrams of Figs. 15(a)–15(c) are the same as (A6).

The two-loop diagrams of Figs. 15(d)–15(h) are

$$\mathcal{V}^{(d)} = \frac{e^2 M^2 T^2}{8(4\pi)^2} \left[\frac{1}{\bar{\epsilon}} - \frac{2}{3} \right] + \mathcal{O}(e^5 T^4), \quad (\text{A10d})$$

$$\mathcal{V}^{(e)} = \frac{e^2 (3e^2 - g_Y^2) \phi^2 T^2}{8(4\pi)^2} \left[\frac{1}{\bar{\epsilon}} - \frac{2}{3} \right] + \mathcal{O}(e^5 T^4), \quad (\text{A10e})$$

$$\mathcal{V}^{(f)} = \mathcal{O}(e^5 T^4), \quad (\text{A10f})$$

$$\mathcal{V}^{(g)} = \frac{(3e^4 - g_Y^4) \phi^2 T^2}{6(4\pi)^2} \frac{1}{\bar{\epsilon}} + \mathcal{O}(e^{11/2} T^4), \quad (\text{A10g})$$

$$\mathcal{V}^{(h)} = \frac{e^2 M_L T^3}{16\pi} + \frac{(3e^2 + g_Y^2)}{96\pi} (\tilde{m}_1 + \tilde{m}_2) T^3 + \mathcal{O}(e^{9/2} T^4). \quad (\text{A10h})$$

The two-loop diagrams of Fig. 19 are

$$\mathcal{V}^{(i)} = -\frac{1}{2} e^2 \mathcal{D}_{ffV}(m_f, m_f, M), \quad (\text{A10i})$$

$$\mathcal{V}^{(j)} = -\frac{1}{4} g_Y^2 \mathcal{D}_{ffS}(m_f, m_f, m_1) - \frac{1}{4} g_Y^2 \mathcal{D}_{ffS}(m_f, m_f, m_2), \quad (\text{A10j})$$

$$V^{(k)} = \frac{g_Y^2 m_f^2 T^2}{12(4\pi)^2} \left[\frac{1}{\epsilon} - 2 \ln 2 \right] + O(e^6 T^4), \quad (\text{A10k})$$

$$V^{(l)} = 0. \quad (\text{A10l})$$

3. Gauged SU(2) Higgs theory

Take $g_s = g_Y = g_1 = e = \theta_W = \bar{\theta} = 0$; set $M_Z = M_W = M$, $M_{LZ} = M_{LW} = M_L$, $g_2 = g$; and ignore M_{LY} in the minimal standard model results below.

4. Minimal standard model

Counterterms:

$$\begin{aligned} \phi_{\text{bare}} &= \left[1 + \frac{9g_2^2 + 3g_1^2 - 12g_Y^2}{8(4\pi)^2 \epsilon} + \dots \right] \phi, \\ A_{\text{bare}} &= \left[1 + \left[\frac{25}{12} - \frac{2n_f}{3} \right] \frac{g_2^2}{(4\pi)^2 \epsilon} + \dots \right] A, \\ B_{\text{bare}} &= \left[1 - \left[\frac{1}{12} + \frac{10n_f}{9} \right] \frac{g_1^2}{(4\pi)^2 \epsilon} + \dots \right] B, \\ t_{L,\text{bare}} &= \left[1 - \frac{g_Y^2}{4(4\pi)^2 \epsilon} + \dots \right] \psi_L, \\ t_{R,\text{bare}} &= \left[1 - \frac{g_Y^2}{2(4\pi)^2 \epsilon} + \dots \right] \psi_R, \\ g_{2,\text{bare}}^2 &= \left[1 - \left[\frac{43}{6} - \frac{4n_f}{3} \right] \frac{g_2^2}{(4\pi)^2 \epsilon} + \dots \right] g_2^2 \mu^{2\epsilon}, \\ g_{1,\text{bare}}^2 &= \left[1 + \left[\frac{1}{6} + \frac{20n_f}{9} \right] \frac{g_1^2}{(4\pi)^2 \epsilon} + \dots \right] g_1^2 \mu^{2\epsilon}, \\ g_{Y,\text{bare}} &= \left[1 + \left[\frac{9}{4} g_Y^2 - 4g_s^2 - \frac{9}{8} g_2^2 - \frac{17}{24} g_1^2 \right] \frac{1}{(4\pi)^2 \epsilon} + \dots \right] g_Y \mu^\epsilon, \\ \lambda_{\text{bare}} &= \left[1 + \left[\frac{27}{8} g_2^4 + \frac{9}{4} g_2^2 g_1^2 + \frac{9}{8} g_1^4 - 18g_Y^4 \right] \frac{1}{(4\pi)^2 \epsilon} + \dots \right] \lambda \mu^{2\epsilon}, \\ v_{\text{bare}}^2 &= \left[1 - \frac{9g_2^2 + 3g_1^2 - 12g_Y^2}{4(4\pi)^2 \epsilon} + \dots \right] v^2. \end{aligned} \quad (\text{A11})$$

Formulas for running couplings may be obtained as in Sec. A1.

Masses:

$$M_W^2 = \frac{1}{4} g_2^2 \phi^2, \quad M_Z^2 = \frac{1}{4} (g_2^2 + g_1^2) \phi^2, \quad m_f^2 = \frac{1}{2} g_Y^2 \phi^2, \quad (\text{A12})$$

$$m_1^2 = -v^2 + \frac{1}{2} \lambda \phi^2, \quad m_2^2 = -v^2 + \frac{1}{6} \lambda \phi^2, \quad (\text{A13})$$

$$M_{LW}^2 = \frac{1}{4} g_2^2 \phi^2 + \left[\frac{5}{6} + \frac{n_f}{3} \right] g_2^2 T^2, \quad (\text{A14})$$

$$\bar{m}_i^2 = m_i^2 + \left[\lambda + \frac{9}{4} g_2^2 + \frac{3}{4} g_1^2 + 3g_Y^2 \right] \frac{T^2}{12} + \dots. \quad (\text{A15})$$

$$\begin{pmatrix} \frac{1}{4}g_2^2\phi^2 + \left[\frac{5}{6} + \frac{n_f}{3}\right]g_2^2T^2 & -\frac{1}{4}g_1g_2\phi^2 \\ -\frac{1}{4}g_1g_2\phi^2 & \frac{1}{4}g_1^2\phi^2 + \left[\frac{1}{6} + \frac{5n_f}{9}\right]g_1^2T^2 \end{pmatrix} \equiv \begin{pmatrix} \cos\tilde{\theta} & \sin\tilde{\theta} \\ -\sin\tilde{\theta} & \cos\tilde{\theta} \end{pmatrix} \begin{pmatrix} M_{LZ}^2 & \\ & M_{L\gamma}^2 \end{pmatrix} \begin{pmatrix} \cos\tilde{\theta} & -\sin\tilde{\theta} \\ \sin\tilde{\theta} & \cos\tilde{\theta} \end{pmatrix}. \quad (\text{A16})$$

The one-loop result is

$$\begin{aligned} \mathcal{V}^{(1)} = & \frac{1}{2} \left[-v^2 + \left[\lambda + \frac{9}{4}g_2^2 + \frac{3}{4}g_1^2 + 3g_Y^2 \right] \frac{T^2}{12} \right] \phi^2 - \frac{1}{12\pi} (4M_W^3 + 2M_Z^3 + 2M_{LW}^3 + M_{LZ}^3 + M_{L\gamma}^3) T + \frac{1}{4!} \lambda \phi^4 \\ & - \frac{3(2M_W^4 + M_Z^4)}{4(4\pi)^2} \left[\ln \left[\frac{\bar{\mu}^2}{T^2} \right] - \frac{2}{3} - 2c_B \right] + \frac{3m_f^4}{(4\pi)^2} \left[\ln \left[\frac{\bar{\mu}^2}{T^2} \right] - 2c_F \right] + \mathcal{O}(g^{9/2}T^4). \end{aligned} \quad (\text{A17})$$

The two-loop diagrams of Fig. 23 are as follows.

$\cos\theta_w$ is defined below by the tree-level relation $\tan\theta_w = g_1/g_2$, and e is $g_2\sin\theta_w$. We shall also use the short-hand notation

$$\begin{aligned} \Delta\mathcal{M}_2 &= 2M_{LW} + M_{LZ}\cos^2\tilde{\theta} + M_{L\gamma}\sin^2\tilde{\theta} - 2M_W - M_Z\cos^2\theta_w, \\ \Delta\mathcal{M}_1 &= M_{LZ}\sin^2\tilde{\theta} + M_{L\gamma}\cos^2\tilde{\theta} - M_Z\sin^2\theta_w. \end{aligned} \quad (\text{A18})$$

Take care to note that many of the graphs below are written in terms of the \mathcal{D}^R instead of the \mathcal{D} . This is because of notational complications caused by the difference between θ_w and $\tilde{\theta}$:

$$\begin{aligned} \mathcal{V}^{(a)} = & -\frac{1}{4}g_2^2\mathcal{D}_{SSV}^R(m_1, m_2, M_W) - \frac{1}{4}g_2^2\mathcal{D}_{SSV}^R(m_2, m_2, M_W) \\ & - \frac{1}{8} \frac{g_2^2}{\cos^2\theta_w} \mathcal{D}_{SSV}^R(m_1, m_2, M_Z) - \frac{1}{8} \frac{g_2^2}{\cos^2\theta_w} (1 - 2\sin^2\theta_w)^2 \mathcal{D}_{SSV}^R(m_2, m_2, M_Z) \\ & - \frac{1}{2} e^2 \mathcal{D}_{SSV}^R(m_2, m_2, 0) - \frac{T^3}{96\pi} (g_2^2\Delta\mathcal{M}_2 + g_1^2\Delta\mathcal{M}_1) + \mathcal{O}(g^{9/2}T^4), \end{aligned} \quad (\text{A19a})$$

$$\begin{aligned} \mathcal{V}^{(b)} = & -\phi^2 \left\{ \frac{1}{32} g_2^4 \mathcal{D}_{SVV}(m_1, M_W, M_W) + \frac{1}{64} \frac{g_2^4}{\cos^4\theta_w} [\mathcal{D}_{SVV}^R(m_1, M_Z, M_Z) - 4\bar{H}_3(m_1, M_Z, M_Z)] \right. \\ & + \frac{1}{16} g_2^2 e^2 \tan^2\theta_w [\mathcal{D}_{SVV}^R(m_2, M_W, M_Z) - 4\bar{H}_3(m_2, M_W, M_Z)] \\ & + \frac{1}{16} g_2^2 e^2 [\mathcal{D}_{SVV}^R(m_2, M_W, 0) - 4\bar{H}_3(m_2, M_W, 0)] + \frac{1}{16} (g_2\cos\tilde{\theta} + g_1\sin\tilde{\theta})^4 \bar{H}_3(m_1, M_{LZ}, M_{LZ}) \\ & + \frac{1}{8} (g_2\cos\tilde{\theta} + g_1\sin\tilde{\theta})^2 (g_2\sin\tilde{\theta} - g_1\cos\tilde{\theta})^2 \bar{H}_3(m_1, M_{LZ}, M_{L\gamma}) \\ & + \frac{1}{16} (g_2\sin\tilde{\theta} - g_1\cos\tilde{\theta})^4 \bar{H}_3(m_1, M_{L\gamma}, M_{L\gamma}) + \frac{1}{4} g_2^2 g_1^2 \sin^2\tilde{\theta} \bar{H}_3(m_2, M_{LW}, M_{LZ}) \\ & \left. + \frac{1}{4} g_2^2 g_1^2 \cos^2\tilde{\theta} \bar{H}_3(m_2, M_{LW}, M_{L\gamma}) \right\} + \mathcal{O}(g^5T^4), \end{aligned} \quad (\text{A19b})$$

$$\begin{aligned} \mathcal{V}^{(c)} = & -\frac{1}{4}g_2^2\mathcal{D}_{SV}^R(m_2, M_W) - \frac{1}{8}g_2^2[\mathcal{D}_{SV}^R(m_1, M_W) + \mathcal{D}_{SV}^R(m_2, M_W)] \\ & - \frac{1}{8} \frac{g_2^2}{\cos^2\theta_w} (1 - 2\sin^2\theta_w)^2 \mathcal{D}_{SV}^R(m_2, M_Z) - \frac{1}{2} e^2 \mathcal{D}_{SV}^R(m_2, 0) \\ & - \frac{1}{16} \frac{g_2^2}{\cos^2\theta_w} [\mathcal{D}_{SV}^R(m_1, M_Z) + \mathcal{D}_{SV}^R(m_2, M_Z)] - \frac{T^3}{96\pi} (g_2^2\Delta\mathcal{M}_2 + g_1^2\Delta\mathcal{M}_1) \\ & - \left[\frac{3}{4}g_2^2 + \frac{1}{4}g_1^2 \right] (\bar{m}_1 - m_1 + 3\bar{m}_2 - 3m_2) \frac{T^3}{32\pi} + \mathcal{O}(g^{9/2}T^4), \end{aligned} \quad (\text{A19c})$$

$$\mathcal{V}^{(d)} = \frac{T^2}{4(4\pi)^2} \left[g_1^2 M_Z^2 \sin^2\theta_w \left[\frac{1}{12} + \frac{10n_f}{9} \right] - 3g_2^2 M_W^2 \left[\frac{25}{12} - \frac{2n_f}{3} \right] \right] \left[\frac{1}{\bar{\epsilon}} - \frac{2}{3} \right] + \mathcal{O}(g^5T^4), \quad (\text{A19d})$$

$$V^{(e)} = -\frac{3\phi^2 T^2}{128(4\pi)^2} (3g_2^4 - 6g_2^2 g_1^2 - g_1^4 + 12g_2^2 g_Y^2 + 4g_1^2 g_Y^2) \left[\frac{1}{\bar{\epsilon}} - \frac{2}{3} \right] + O(g^{9/2} T^4), \quad (\text{A19e})$$

$$V^{(f)} = O(g^5 T^4), \quad (\text{A19f})$$

$$V^{(g)} = \left[\frac{9}{8} g_2^4 + \frac{3}{4} g_2^2 g_1^2 + \frac{3}{8} g_1^4 - 6g_Y^4 \right] \frac{\phi^2 T^2}{8(4\pi)^2} \frac{1}{\bar{\epsilon}} + O(g^{9/2} T^4), \quad (\text{A19g})$$

$$V^{(h)} = g_2^2 \left[\frac{5}{6} + \frac{n_f}{3} \right] (2M_{LW} + \cos^2 \bar{\theta} M_{LZ} + \sin^2 \bar{\theta} M_{LY}) \frac{T^3}{8\pi} + g_1^2 \left[\frac{1}{6} + \frac{5n_f}{9} \right] (\sin^2 \bar{\theta} M_{LZ} + \cos^2 \bar{\theta} M_{LY}) \frac{T^3}{8\pi} \\ + \left[\frac{3}{4} g_2^2 + \frac{1}{4} g_1^2 + g_Y^2 \right] (\bar{m}_1 + 3\bar{m}_2) \frac{T^3}{32\pi} + O(g^{9/2} T^4), \quad (\text{A19h})$$

$$V^{(i)} = -4g_s^2 \mathcal{D}_{ffV}^R(m_f, m_f, 0) - \frac{3}{16} \frac{g_2^2}{\cos^2 \theta_W} \left[\left[1 - \frac{8}{3} \sin^2 \theta_W \right]^2 + 1 \right] [\mathcal{D}_{ffV}^R(m_f, m_f, M_Z) - \mathcal{D}_{ffV}^R(0, 0, M_Z)] \\ - \frac{3}{2} g_2^2 [\mathcal{D}_{ffV}^R(m_f, 0, M_W) - \mathcal{D}_{ffV}^R(0, 0, M_W)] - 2n_f g_2^2 \mathcal{D}_{ffV}^R(0, 0, M_W) \\ - n_f g_2^2 \left[\cos^2 \theta_W + \frac{5}{3} \frac{\sin^4 \theta_W}{\cos^2 \theta_W} \right] \mathcal{D}_{ffV}^R(0, 0, M_Z) - \frac{4}{3} e^2 \mathcal{D}_{ffV}^R(m_f, m_f, 0) \\ - \frac{n_f T^3}{24\pi} \left[g_2^2 \Delta \mathcal{M}_2 + \frac{5}{3} g_1^2 \Delta \mathcal{M}_1 \right] + O(g^5 T^4), \quad (\text{A19i})$$

$$V^{(j)} = -\frac{3}{4} g_Y^2 \mathcal{D}_{ffS}(m_f, m_f, m_1) - \frac{3}{4} g_Y^2 \mathcal{D}_{ffS}(m_f, m_f, m_2) - \frac{3}{2} g_Y^2 \mathcal{D}_{ffS}(m_f, 0, m_2), \quad (\text{A19j})$$

$$V^{(k)} = \frac{3g_Y^2 m_f^2 T^2}{8(4\pi)^2} \left[\frac{1}{\bar{\epsilon}} - 2 \ln 2 \right] + O(g^6 T^4), \quad (\text{A19k})$$

$$V^{(l)} = -\left[g_s^2 - \frac{1}{12} g_1^2 \right] \frac{\sqrt{2} g_Y m_f \phi T^2}{(4\pi)^2} \left[\frac{1}{\bar{\epsilon}} - 2 \ln 2 \right] + O(g^6 T^4), \quad (\text{A19l})$$

$$V^{(m)} = -\frac{1}{2} g_2^2 \cos^2 \theta_W \mathcal{D}_{VVV}^R(M_W, M_W, M_Z) - \frac{1}{2} e^2 \mathcal{D}_{VVV}^R(M_W, M_W, 0) \\ - \frac{1}{2} g_2^2 \cos^2 \theta_W [\mathcal{D}_{LLT}(M_{LW}, M_{LW}, M_Z) - \mathcal{D}_{LLT}(M_W, M_W, M_Z)] \\ - \frac{1}{2} e^2 [\mathcal{D}_{LLT}(M_{LW}, M_{LW}, 0) - \mathcal{D}_{LLT}(M_W, M_W, 0)] \\ - g_2^2 \cos^2 \bar{\theta} \mathcal{D}_{LLT}(M_{LW}, M_{LZ}, M_W) + g_2^2 \cos^2 \theta_W \mathcal{D}_{LLT}(M_W, M_Z, M_W) \\ - g_2^2 \sin^2 \bar{\theta} \mathcal{D}_{LLT}(M_{LW}, M_{LY}, M_W) + g_2^2 \sin^2 \theta_W \mathcal{D}_{LLT}(M_{LW}, 0, M_W) - \frac{g_2^2 T^3}{16\pi} \Delta \mathcal{M}_2 + O(g^5 T^4), \quad (\text{A19m})$$

$$V^{(n)} = -2g_2^2 \mathcal{D}_{\eta\eta V}^R(M_W) - g_2^2 \cos^2 \theta_W \mathcal{D}_{\eta\eta V}^R(M_Z) + \frac{g_2^2 T^3}{96\pi} \Delta \mathcal{M}_2 + O(g^5 T^4), \quad (\text{A19n})$$

$$V^{(o)} = -\frac{1}{4} g_2^2 \mathcal{D}_{VV}^R(M_W, M_W) - \frac{1}{2} g_2^2 \cos^2 \theta_W \mathcal{D}_{VV}^R(M_W, M_Z) - \frac{1}{2} e^2 \mathcal{D}_{VV}^R(M_W, 0) \\ - \frac{g_2^2 T^3}{32\pi} \Delta \mathcal{M}_2 + \frac{2g_2^2 T^2}{(4\pi)^2} M_W \Delta \mathcal{M}_2 + O(g^5 T^4). \quad (\text{A19o})$$

5. Results for resummed graphs in terms of unresummed graphs

$$\mathcal{D}_{SSV}(m_1, m_2, M) = \mathcal{D}_{SSV}^R(m_1, m_2, M) + \frac{1}{24\pi} (M_L - M) T^3 + O(g^{5/2} T^4), \quad (\text{A20})$$

$$\mathcal{D}_{SVV}(m, M_1, M_2) = \mathcal{D}_{SVV}^R(m, M_1, M_2) + 4\bar{H}_3(\bar{m}, M_{L1}, M_{L2}) - 4\bar{H}_3(m, M_1, M_2) + O(g T^2), \quad (\text{A21})$$

$$\mathcal{D}_{SV}(m, M) = \mathcal{D}_{SV}^R(m, M) + \frac{1}{24\pi}(M_L - M)T^3 + \frac{1}{8\pi}(\tilde{m} - m)T^3 + \mathcal{O}(g^{5/2}T^4), \quad (\text{A22})$$

$$\mathcal{D}_{ffV}(m_{f2}, m_{f1}, M) = \mathcal{D}_{ffV}^R(m_{f2}, m_{f1}, M) + \frac{1}{24\pi}(M_L - M)T^3 + \mathcal{O}(g^3T^4), \quad (\text{A23})$$

$$\mathcal{D}_{ffS}(m_{f2}, m_{f1}, m) = \mathcal{D}_{ffS}^R(m_{f2}, m_{f1}, m) + \frac{1}{24\pi}(\tilde{m} - m)T^3 + \mathcal{O}(g^{7/2}T^4), \quad (\text{A24})$$

$$\begin{aligned} \mathcal{D}_{VVV}(M_1, M_2, M_3) &= \mathcal{D}_{VVV}^R(M_1, M_2, M_3) + \frac{1}{8\pi}(M_{L1} + M_{L2} + M_{L3} - M_1 - M_2 - M_3)T^3 \\ &\quad + \frac{1}{2} \sum_{\text{perms}} [\mathcal{D}_{LLT}(M_{L1}, M_{L2}, M_{L3}) - \mathcal{D}_{LLT}(M_1, M_2, M_3)] + \mathcal{O}(g^3T^4). \end{aligned} \quad (\text{A25})$$

The sum above is over all six permutations of (M_1, M_2, M_3) .

$$\begin{aligned} \mathcal{D}_{LLT}(M_1, M_2, M_3) &= \frac{T^2}{(4\pi)^2} \left[(M_1 + M_2)M_3 - M_1M_2 + \frac{(M_1 + M_2)(M_1 - M_2)^2}{M_3} \right] \\ &\quad + (M_3^2 - 2M_1^2 - 2M_2^2)\bar{H}_3(M_1, M_2, M_3) + \frac{(M_1^2 - M_2^2)^2}{M_3^3} [\bar{H}_3(M_1, M_2, M_3) - \bar{H}_3(M_1, M_2, 0)], \end{aligned} \quad (\text{A26})$$

$$\mathcal{D}_{\eta\eta V}(M) = \mathcal{D}_{\eta\eta V}^R(M) - \frac{1}{96\pi}(M_L - M)T^3 + \mathcal{O}(g^3T^4), \quad (\text{A27})$$

$$\begin{aligned} \mathcal{D}_{VV}(M_1, M_2) &= \mathcal{D}_{VV}^R(M_1, M_2) + \frac{1}{16\pi}(M_{L1} + M_{L2} - M_1 - M_2)T^3 \\ &\quad - [(M_{L1} - M_1)M_2 + M_1(M_{L2} - M_2)] \frac{4T^2}{(4\pi)^2} + \mathcal{O}(g^3T^4). \end{aligned} \quad (\text{A28})$$

6. Exact results for unresummed graphs in terms of I , \bar{H} , and L

This section is included only for completeness. The expansions for the \mathcal{D} 's that give our final result for the effective potential through $\mathcal{O}(g^4T^4)$ are given in the next section. We have not bothered to keep track of the \bar{H}_{ff} terms in the fermion contributions below because these do not contribute to the potential at $\mathcal{O}(g^4T^4)$. In the case of \mathcal{D}_{ffS} , these terms in fact depend on whether the S is a scalar or a pseudoscalar—a distinction we are otherwise able to ignore:

$$\begin{aligned} \mathcal{D}_{SSV}^R(m_1, m_2, M) &= I(M)[I(m_1) + I(m_2)] - I(m_1)I(m_2) + (M^2 - 2m_1^2 - 2m_2^2)\bar{H}(m_1, m_2, M) \\ &\quad + \frac{m_1^2 - m_2^2}{M^2} [I(M) - I(0)][I(m_1) - I(m_2)] + \frac{(m_1^2 - m_2^2)^2}{M^2} [\bar{H}(m_1, m_2, M) - \bar{H}(m_1, m_2, 0)], \end{aligned} \quad (\text{A29})$$

$$\begin{aligned} \mathcal{D}_{SVV}^R(m, M_1, M_2) &= \left\{ \frac{1}{M_1^2} [I(M_1) - I(0)][I(M_2) - I(m)] \right. \\ &\quad - \frac{m^2}{2M_1^2 M_2^2} [I(M_1) - I(0)][I(M_2) - I(0)] + (5 - 4\epsilon)\bar{H}(m, M_1, M_2) \\ &\quad + \frac{m^4}{2M_1^2 M_2^2} [\bar{H}(m, M_1, M_2) - 2\bar{H}(m, M_1, 0) + \bar{H}(m, 0, 0)] \\ &\quad \left. + \frac{M_1^2 - 2m^2}{M_2^2} [\bar{H}(m, M_1, M_2) - \bar{H}(m, M_1, 0)] \right\} + \{M_1 \leftrightarrow M_2\}, \end{aligned} \quad (\text{A30})$$

$$\mathcal{D}_{SV}^R(m, M) = -2(3 - 2\epsilon)I(m)I(M), \quad (\text{A31})$$

$$\begin{aligned} \mathcal{D}_{ffV}^R(m_{f2}, m_{f1}, M) &= 2(1 - \epsilon)[I_f(m_{f2}) + I_f(m_{f1})]I(M) - 2(1 - \epsilon)I_f(m_{f2})I_f(m_{f1}) \\ &\quad - \frac{m_{f2}^2 - m_{f1}^2}{M^2} [I_f(m_{f2}) - I_f(m_{f1})][I(M) - I(0)] + \mathcal{O}(g^2T^2\bar{H}_{ff}), \end{aligned} \quad (\text{A32})$$

$$\mathcal{D}_{ffS}^R(m_{f2}, m_{f1}, m) = 2[I_f(m_{f2}) + I_f(m_{f1})]I(m) - 2I_f(m_{f2})I_f(m_{f1}) + \mathcal{O}(g^2T^2\bar{H}_{ff}), \quad (\text{A33})$$

$$\begin{aligned}
\mathcal{D}_{VVV}^R(M_1, M_2, M_3) = & \frac{1}{2} \sum_{\text{perms}} \left\{ \frac{1}{4} \frac{M_1^6}{M_2^2 M_3^2} \bar{H}(M_1, 0, 0) - \frac{1}{4} \frac{M_1^4}{M_2^2 M_3^2} [I(0)]^2 - L(M_1, M_2) \right. \\
& + \left[(-4 + 4\epsilon) \frac{M_1^4}{M_3^2} + \left[\frac{9}{2} - 4\epsilon \right] \frac{M_1^2 M_2^2}{M_3^2} - \frac{1}{2} \frac{M_1^6}{M_2^2 M_3^2} \right] \bar{H}(M_1, M_2, 0) \\
& + \left[\left[\frac{7}{2} - 2\epsilon \right] + \left[\frac{9}{2} - 4\epsilon \right] \left[\frac{M_1^2}{M_2^2} - \frac{M_2^2}{M_1^2} \right] - \frac{1}{4} \frac{M_3^4}{M_1^2 M_2^2} \right] I(M_1) I(M_2) \\
& + \left[\left[\frac{9}{2} - 4\epsilon \right] \left[\frac{M_2^2}{M_3^2} - \frac{M_1^2}{M_2^2} \right] + \frac{1}{2} \frac{M_2^4}{M_1^2 M_3^2} \right] I(M_1) I(0) \\
& \left. + \left[(-8 + 6\epsilon) M_1^2 + (4 - 4\epsilon) \frac{M_1^4}{M_3^2} + \left[-\frac{9}{2} + 4\epsilon \right] \frac{M_1^2 M_2^2}{M_3^2} + \frac{1}{4} \frac{M_1^6}{M_2^2 M_3^2} \right] \bar{H}(M_1, M_2, M_3) \right\}
\end{aligned} \tag{A34}$$

The sum above is over all six permutations of (M_1, M_2, M_3) .

$$\mathcal{D}_{\eta\eta V}(M) = -\frac{1}{2} I(M) I(0) - \frac{1}{4} M^2 \bar{H}(M, 0, 0), \tag{A35}$$

$$\mathcal{D}_{VV}^R(M_1, M_2) = 2L(M_1, M_2) + (-14 + 20\epsilon) I(M_1) I(M_2). \tag{A36}$$

7. Expansion of results for unresummed graphs

$$\mathcal{D}_{SSV}^R(m_1, m_2, M) = -\frac{MT^3}{24\pi} + \frac{M^2 T^2}{(4\pi)^2} \left[\frac{1}{12} \frac{1}{\bar{\epsilon}} + \frac{1}{12} \ln \left[\frac{\bar{\mu}^2}{T^2} \right] + \ln \left[\frac{3T}{M} \right] + \frac{1}{2} + \frac{1}{3} c_B - \frac{1}{4} c_H \right] + \mathcal{O}(g^{5/2} T^4), \tag{A37}$$

$$\begin{aligned}
\mathcal{D}_{SVV}^R(m, M_1, M_2) = & \frac{T^2}{(4\pi)^2} \left[\frac{5}{2} \frac{1}{\bar{\epsilon}} + \frac{5}{2} \ln \left[\frac{\bar{\mu}^2}{T^2} \right] + 3 - \frac{5}{2} c_H + \frac{M_1}{M_2} + \frac{M_2}{M_1} + \left[10 + \frac{M_1^2}{M_2^2} + \frac{M_2^2}{M_1^2} \right] \ln \left[\frac{3T}{M_1 + M_2} \right] \right. \\
& \left. - \frac{M_1^2}{M_2^2} \ln \left[\frac{3T}{M_1} \right] - \frac{M_2^2}{M_1^2} \ln \left[\frac{3T}{M_2} \right] \right] + \mathcal{O}(g^{1/2} T^2),
\end{aligned} \tag{A38}$$

$$\mathcal{D}_{SV}^R(m, M) = \frac{M^2 T^2}{(4\pi)^2} \left[\frac{1}{2} \frac{1}{\bar{\epsilon}} + \frac{1}{2} \ln \left[\frac{\bar{\mu}^2}{T^2} \right] - \frac{1}{3} - c_B \right] + \frac{MT^3}{8\pi} + \frac{mT^3}{8\pi} + \mathcal{O}(g^{7/2} T^4), \tag{A39}$$

$$\begin{aligned}
\mathcal{D}_{ffV}^R(m_{f_2}, m_{f_1}, M) = & \frac{(m_{f_2}^2 + m_{f_1}^2) T^2}{(4\pi)^2} \left[-\frac{1}{4} \frac{1}{\bar{\epsilon}} - \frac{1}{4} \ln \left[\frac{\bar{\mu}^2}{T^2} \right] + \frac{1}{4} + \frac{1}{2} c_F + \frac{1}{6} \ln 2 \right] \\
& + \frac{M^2 T^2}{(4\pi)^2} \left[\frac{1}{6} \frac{1}{\bar{\epsilon}} + \frac{1}{6} \ln \left[\frac{\bar{\mu}^2}{T^2} \right] - \frac{1}{6} - \frac{1}{3} c_B - \frac{1}{3} \ln 2 \right] + \frac{MT^3}{24\pi} + \mathcal{O}(g^3 T^4),
\end{aligned} \tag{A40}$$

$$\mathcal{D}_{ffS}^R(m_{f_2}, m_{f_1}, m) = \frac{(m_{f_2}^2 + m_{f_1}^2) T^2}{(4\pi)^2} \left[-\frac{1}{4} \frac{1}{\bar{\epsilon}} - \frac{1}{4} \ln \left[\frac{\bar{\mu}^2}{T^2} \right] + \frac{1}{2} c_F + \frac{1}{6} \ln 2 \right] + \frac{mT^3}{24\pi} + \mathcal{O}(g^{7/2} T^4), \tag{A41}$$

$$\begin{aligned}
\mathcal{D}_{VVV}^R(M, M, M_3) = & \frac{T^2}{(4\pi)^2} \left[(2M^2 + M_3^2) \left[-\frac{61}{24} \frac{1}{\bar{\epsilon}} - \frac{61}{24} \ln \frac{\bar{\mu}^2}{T^2} + \frac{13}{8} + \frac{13}{12} c_B + 2c_H \right] \right. \\
& + \frac{11}{6} M M_3 - \frac{25}{3} M_3^2 + \frac{9M_3^3}{2M} - \frac{M^3}{2M_3} - \frac{M_3^4}{4M^2} \\
& + \left[-4M^2 + 9M_3^2 - \frac{M^4}{2M_3^2} - \frac{4M_3^4}{M^2} - \frac{M_3^6}{2M^4} \right] \ln \left[\frac{3T}{M + M_3} \right] \\
& + \left[-12M^2 - 17M_3^2 + \frac{4M_3^4}{M^2} + \frac{M_3^6}{4M^4} \right] \ln \left[\frac{3T}{2M + M_3} \right] \\
& \left. + \frac{M^4}{2M_3^2} \ln \left[\frac{3T}{M} \right] + \frac{M_3^6}{4M^4} \ln \left[\frac{3T}{M_3} \right] \right] - (2M + M_3) \frac{T^3}{8\pi} + \mathcal{O}(g^3 T^4),
\end{aligned} \tag{A42}$$

$$\mathcal{D}_{\eta\nu}^{\mathcal{R}}(M) = \frac{M^2 T^2}{(4\pi)^2} \left[-\frac{1}{48} \frac{1}{\bar{\epsilon}} - \frac{1}{48} \ln \frac{\bar{\mu}^2}{T^2} - \frac{1}{8} - \frac{1}{12} c_B + \frac{1}{16} c_H - \frac{1}{4} \ln \left[\frac{3T}{M} \right] \right] + \frac{MT^3}{96\pi} + \mathcal{O}(g^3 T^4), \quad (\text{A43})$$

$$\mathcal{D}_{\nu\nu}^{\mathcal{R}}(M_1, M_2) = \frac{T^2}{(4\pi)^2} \left[(M_1^2 + M_2^2) \left[\frac{9}{8} \frac{1}{\bar{\epsilon}} + \frac{9}{8} \ln \frac{\bar{\mu}^2}{T^2} - \frac{13}{8} - \frac{9}{4} c_B \right] - \frac{40}{3} M_1 M_2 \right] + \frac{13}{48\pi} (M_1 + M_2) T^3 + \mathcal{O}(g^3 T^4). \quad (\text{A44})$$

8. Some useful limits

$$\mathcal{D}_{VVV}^{\mathcal{R}}(M, M, 0) = \frac{M^2 T^2}{(4\pi)^2} \left[-\frac{61}{12} \frac{1}{\bar{\epsilon}} - \frac{61}{12} \ln \frac{\bar{\mu}^2}{T^2} + 3 + \frac{13}{6} c_B + 4c_H + 12 \ln 2 - 16 \ln \left[\frac{3T}{M} \right] \right] + \mathcal{O}(g^3 T^4), \quad (\text{A45})$$

$$\mathcal{D}_{SVV}^{\mathcal{R}}(m, M, 0) = \frac{T^2}{(4\pi)^2} \left[\frac{5}{2} \frac{1}{\bar{\epsilon}} + \frac{5}{2} \ln \frac{\bar{\mu}^2}{T^2} + \frac{7}{2} - \frac{5}{2} c_H + 10 \ln \left[\frac{3T}{M} \right] \right] + \mathcal{O}(g^{1/2} T^2), \quad (\text{A46})$$

$$\mathcal{D}_{LLT}^{\mathcal{R}}(M_1, M_2, 0) = \frac{T^2}{(4\pi)^2} \left[\frac{1}{2} M_1^2 - 2M_1 M_2 + \frac{1}{2} M_2^2 \right] - 2(M_1^2 + M_2^2) \bar{H}_3(M_1, M_2, 0). \quad (\text{A47})$$

APPENDIX B: DERIVATION OF SOME HIGH-TEMPERATURE EXPANSIONS

1. Expansion of \bar{H}_{ff}

In this appendix, we shall derive the leading $\mathcal{O}(T^2)$ term in the high-temperature expansion of $\bar{H}_{ff}(m_{f_2}, m_{f_1}; m)$, defined by (5.12). Because two of the three Euclidean momenta $P, Q, P+Q$ are fermionic, \bar{H}_{ff} does not diverge in the infrared if we set all the masses to zero. So the leading $\mathcal{O}(T^2)$ term is simply

$$\bar{H}_{ff}(m_{f_2}, m_{f_1}; m) = \mu^{4\epsilon} \mathfrak{F}_P^{(f)} \mathfrak{F}_Q^{(f)} \frac{1}{P^2 Q^2 (P+Q)^2} + \mathcal{O}(mT). \quad (\text{B1})$$

The result found in this appendix is that

$$\mathfrak{F}_P^{(f)} \mathfrak{F}_Q^{(f)} \frac{1}{P^2 Q^2 (P+Q)^2} = \mathcal{O}(\epsilon) \quad (\text{B2})$$

in dimensional regularization and so vanishes when $\epsilon \rightarrow 0$.

We begin by rewriting the integral in (B2) as

$$T^2 \sum_{\substack{\text{odd} \\ n}} \sum_{\substack{\text{odd} \\ j}} \sum_{\substack{\text{even} \\ k}} \delta_{n+j+k} \int \frac{d^{3-2\epsilon} p}{(2\pi)^{3-2\epsilon}} \frac{d^{3-2\epsilon} q}{(2\pi)^{3-2\epsilon}} \frac{d^{3-2\epsilon} r}{(2\pi)^{3-2\epsilon}} \delta(p+q+r) \frac{1}{[(n\pi T)^2 + p^2][(j\pi T)^2 + q^2][(k\pi T)^2 + r^2]}. \quad (\text{B3})$$

Using the symmetry of this expression, one may replace

$$\sum_{\text{odd}} \sum_{\text{odd}} \sum_{\text{even}} \rightarrow \frac{1}{3} \left[\sum_{\text{any}} \sum_{\text{any}} \sum_{\text{any}} - \sum_{\text{even}} \sum_{\text{even}} \sum_{\text{even}} \right], \quad (\text{B4})$$

where we will restrict the triple sum on the right-hand side to exclude the case $(n, j, l) = (0, 0, 0)$ where all the frequencies are simultaneously zero. By scaling all three-momenta by a factor of 2 in the first term on the right-hand side of (B4), we obtain

$$\sum_{\text{odd}} \sum_{\text{odd}} \sum_{\text{even}} \rightarrow \frac{2^{4\epsilon} - 1}{3} \sum_{\text{even}} \sum_{\text{even}} \sum_{\text{even}}. \quad (\text{B5})$$

So we may relate \bar{H}_{ff} to something resembling the bosonic function \bar{H} :

$$\mathfrak{F}_P^{(f)} \mathfrak{F}_Q^{(f)} \frac{1}{P^2 Q^2 (P+Q)^2} = \epsilon \left[\frac{4}{3} \ln 2 + \mathcal{O}(\epsilon) \right] \mathfrak{F}_P \mathfrak{F}_Q \frac{1 - \delta_{p_0} \delta_{q_0}}{P^2 Q^2 (P+Q)^2}. \quad (\text{B6})$$

The result will be nonzero when $\epsilon \rightarrow 0$ only if the bosonic integrals on the right-hand side give a divergent contribution of order $1/\epsilon$. To relate this result more directly to the bosonic function $H(m)$, we need to temporarily put in an infrared cutoff m :

$$\int_P \int_Q \frac{1 - \delta_{p_0} \delta_{q_0}}{P^2 Q^2 (P+Q)^2} = \lim_{m \rightarrow 0} \left\{ H(m) - T^2 \int \frac{d^{3-2\epsilon} p}{(2\pi)^{3-2\epsilon}} \frac{d^{3-2\epsilon} q}{(2\pi)^{3-2\epsilon}} \frac{1}{(p^2 + m^2)(q^2 + m^2)[(p+q)^2 + m^2]} \right\}. \quad (\text{B7})$$

It is straightforward to compute the $1/\epsilon$ term of the above three-dimensional integrals using standard techniques for loop integrals. One finds that it exactly cancels the $1/\epsilon$ piece of $H(m)$ shown in (3.17), from which (B2) then follows.

2. Expansion of $L(m_1, m_2)$

Working from the definition (6.3) of $L(m_1, m_2)$,

$$\begin{aligned} L(m_1, m_2) &= \int \frac{p_0^2}{P^2(P^2 + m_1^2)} \int \frac{q_0^2}{Q^2(Q^2 + m_2^2)} + \sum_{i,j=1}^{3-2\epsilon} \int \frac{p_i p_j}{P^2(P^2 + m_1^2)} \int \frac{q_i q_j}{Q^2(Q^2 + m_2^2)} \\ &= \int \frac{p_0^2}{P^2(P^2 + m_1^2)} \int \frac{q_0^2}{Q^2(Q^2 + m_2^2)} + \frac{1}{(3-2\epsilon)} \left[I(m_1) - \int \frac{p_0^2}{P^2(P^2 + m_1^2)} \right] \left[I(m_2) - \int \frac{p_0^2}{P^2(P^2 + m_2^2)} \right]. \end{aligned} \quad (\text{B8})$$

An expansion for the remaining integral may easily be found by the method of (3.32):

$$\int \frac{p_0^2}{P^2(P^2 + m^2)} = -\frac{1}{24} T^2 - \frac{1}{64\pi^2} m^2 \left[\frac{1}{\epsilon} + \ln \left[\frac{\bar{\mu}^2}{T^2} \right] - 2c_B + 2 \right] + O(m^4/T^2) - \epsilon(\nu_\epsilon - 2) \frac{1}{24} T^2 + O(\epsilon m^2). \quad (\text{B9})$$

The high-temperature expansion of $L(m_1, m_2)$ is then

$$L(m_1, m_2) = \text{const} - \frac{(m_1 + m_2) T^3}{24 \times 4\pi} - (m_1^2 + m_2^2) \frac{T^2}{48(4\pi)^2} \left[\frac{1}{\epsilon} + \nu_\epsilon + \ln \frac{\bar{\mu}^2}{T^2} - 2c_B - 1 \right] + \frac{m_1 m_2 T^2}{3(4\pi)^2} + O(m^3 T) + O(\epsilon). \quad (\text{B10})$$

APPENDIX C: CRITICISM OF THE SUPERDAISY APPROXIMATION

A previous attempt to compute corrections to the ring-improved one-loop potential in Ref. [14] has relied on the superdaisy approximation to simplify the calculation. In this appendix, we shall explain why the superdaisy approximation does not correctly reproduce the leading corrections to the one-loop potential. The superdaisy approximation is an approximation to Dyson's equations where the effective masses of particles are derived at one loop (to any desired order in M/T) from diagrams such as Figs. 1 and 5, and then those masses are used self-consistently to improve the propagators used to derive the effective masses in the first place. The result is a set of coupled equations which may be solved for the effective masses. In pure scalar theory, for example, the equation is given schematically by Fig. 28 (ignoring renormalization and counterterms):

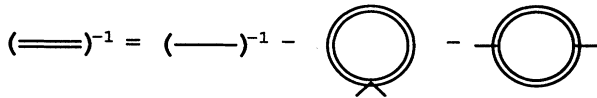
$$(\equiv)^{-1} = (\text{---})^{-1} - \text{---} \text{---} \text{---} - \text{---} \text{---} \text{---}$$


FIG. 28. The one-loop approximation to Dyson's equation for the self-energy.

$$\begin{aligned} m_{\text{eff}}^2 &\approx m^2 + \frac{1}{2} \lambda \int_P \frac{1}{P^2 + m_{\text{eff}}^2} \\ &\quad - \frac{1}{2} \lambda^2 \phi^2 \int_P \frac{1}{(P^2 + m_{\text{eff}}^2)^2}. \end{aligned} \quad (\text{C1})$$

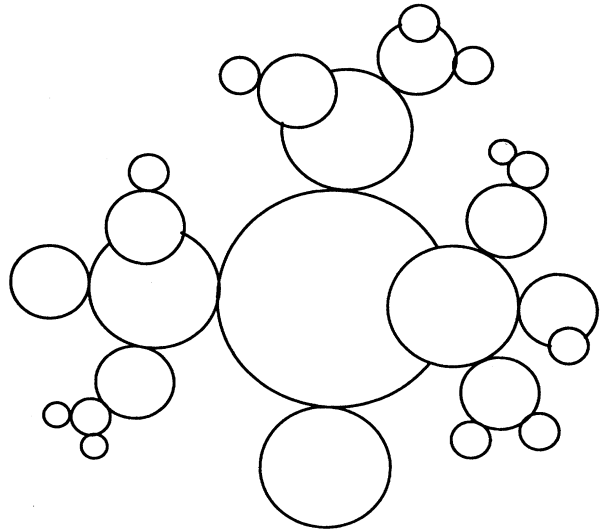


FIG. 29. A generic superdaisy diagram in the pure scalar theory.

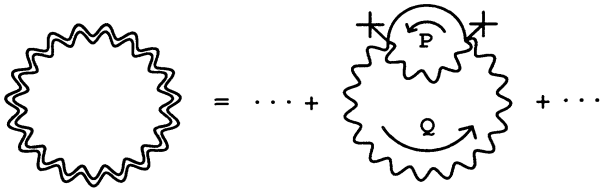


FIG. 30. A disastrous term in the superdaisy resummation of the one-loop vector diagram.

Computing the one-loop potential with these masses is then equivalent to some approximation to the set of superdaisy diagrams, such as shown in Fig. 29.

Superdaisy equations such as (C1), however, do not give adequate approximations to these graphs. (C1) should really read

$$\begin{aligned} \Pi(Q) \approx m^2 + \frac{1}{2} \lambda \oint_P \frac{1}{P^2 + \Pi(P)} \\ - \frac{1}{2} \lambda^2 \phi^2 \oint_P \frac{1}{[P^2 + \Pi(P)][(P+Q)^2 + \Pi(P+Q)]}, \end{aligned} \quad (\text{C2})$$

where $\Pi(P)$ is the one-loop self-energy. The approximation made in (C1) was to replace $\Pi(P)$ by $\Pi(0)$ inside loops. Thus, Fig. 29 has been approximated by first computing the smallest (outermost) loops in the approximation that no momenta flows into them, then computing the next smallest loops in the same approximation, then the next, and so forth. At each stage, the approximation is valid only if the momentum flowing through a loop is small compared to the momenta of all the smaller loops that decorate it. And therein lies the rub. Once quadratically divergent pieces have been accounted for (say, by normal ring resummation as opposed to superdaisy resummation), then most loops are dominated by momenta of order M and there is no hierarchy of momenta in a graph. So, for example, the $O(g^2 M^2 T^2)$ contributions of Fig. 20(m) cannot be correctly computed in an approximation that replaces one loop by $\Pi(0)$.

The problem can be even more egregious if care is not taken to avoid mishandling hard ($P \sim T$) thermal loops. Consider the particular contribution to the superdaisy improved one-loop potential shown on the right-hand side of Fig. 30. The superdaisy approximation instructs us to first evaluate the small loop assuming $Q=0$. This small loop is then dominated by loop momenta P of order M . When we replace the result $\Pi(Q)$ of the small loop by an effective-mass insertion $\Pi(0)$, the large loop becomes

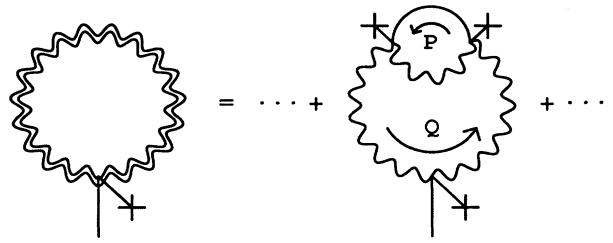


FIG. 31. The tadpole version of Fig. 31, which is still problematical.

quadratically divergent and so is dominated by momenta $Q \sim T$. But this is exactly the *opposite* hierarchy of momenta from the one needed to justify the superdaisy approximation. Reference [14] sidesteps this disaster by computing the derivative of the effective potential rather than the effective potential itself. In the tadpole graph of Fig. 31, the large loop never has momentum T when it is decorated by smaller loops. But this does *not* save the superdaisy approximation. The large loop is now dominated by momenta $Q \sim M$, and the $O(MT)$ corrections from the small loop are also dominated by momenta $P \sim M$; the necessary hierarchy of momenta is still absent.

As discussed in Sec. IV B, there are a few diagrams where there *is* a hierarchy of scales when the scalar mass is much smaller than the vector mass. The resummation discussed in that section does not benefit from the full superdaisy approximation of (C1) and was in any case irrelevant to our final results for the leading corrections to the one-loop potential.

In Sec. IV D, we discussed how the most important terms for shifting the VEV from its one-loop value are those that depend on logarithms of masses. The superdaisy approximation will never generate such terms because it always reduces multiloop diagrams to a hierarchy of one-loop diagrams (with some number of mass insertions) and the result $I(M)$ for a one-loop diagram does not contain any $\ln M$ terms [see (3.12)]. Such terms do appear in many of the expressions in Ref. [14], but this is because there $I(M)$ is routinely split into separate zero-temperature and temperature-dependent pieces. Though each piece depends on $\ln M$, the sum does not. Reference [14] does consider one diagram in addition to the superdaisy one-loop tadpole, and this one diagram will indeed generate some $\ln M$ terms. However, the other $\ln M$ terms from all those diagrams subsumed by the superdaisy one-loop tadpole [such as the derivative of Fig. 21(m), for example] are lost.

- [1] M. Shaposhnikov, Pis'ma Zh. Eksp. Teor. Fiz. **44**, 405 (1986) [JETP Lett. **44**, 521 (1986)]; Nucl. Phys. **B299**, 707 (1988).
 [2] L. McLerran, Phys. Rev. Lett. **62**, 1075 (1989).
 [3] N. Turok and J. Zadrozny, Phys. Rev. Lett. **65**, 2331 (1990); Nucl. Phys. **B358**, 471 (1991); L. McLerran, M.

Shaposhnikov, N. Turok, and M. Voloshin, Phys. Lett. B **256**, 451 (1991).

- [4] A. Cohen, D. Kaplan, and A. Nelson, Phys. Lett. B **245**, 561 (1990); Nucl. Phys. **B349**, 727 (1991); Phys. Lett. B **263**, 86 (1992).
 [5] M. Dine, P. Huet, R. Singleton, and L. Susskind, Phys.

- Lett. B **257**, 351 (1992); M. Dine, P. Huet, and R. Singleton, Nucl. Phys. **B375**, 625 (1992).
- [6] A. Sakharov, Pis'ma Zh. Eksp. Teor. Fiz. **5**, 32 (1967) [JETP Lett. **5**, 24 (1967)].
- [7] F. Klinkhamer and N. Manton, Phys. Rev. D **30**, 2212 (1984).
- [8] V. Kuzmin, V. Rubakov, and M. Shaposhnikov, Phys. Lett. B **308**, 885 (1988).
- [9] P. Arnold and L. McLerran, Phys. Rev. D **37**, 1020 (1988).
- [10] S. Khlebnikov and M. Shaposhnikov, Nucl. Phys. **B308**, 885 (1988).
- [11] M. Shaposhnikov, Phys. Lett. B **277**, 324 (1992); **282**, 483(E) (1992).
- [12] M. Dine, R. Leigh, P. Huet, A. Linde, and D. Linde, Phys. Lett. B **283**, 319 (1992); Phys. Rev. D **46**, 550 (1992).
- [13] T. Mori, in *Proceedings of the XXVIth International Conference on High Energy Physics*, Dallas, Texas, 1992, edited by J. Sanford (AIP, New York, 1993).
- [14] C. G. Boyd, D. Brahm, and S. Hsu, Chicago U. EFI Report No. EFI-92-22, 1992 (unpublished).
- [15] D. A. Kirzhnits and A. D. Linde, Phys. Lett. **42B**, 471 (1972); Ann. Phys. (N.Y.) **101**, 195 (1976).
- [16] S. Weinberg, Phys. Rev. D **9**, 2257 (1974).
- [17] L. Dolan and R. Jackiw, Phys. Rev. D **9**, 3320 (1974).
- [18] K. Takahashi, Z. Phys. C **26**, 601 (1985). The reader should beware that the gauge theory cases are handled incorrectly in this paper.
- [19] P. Fendley, Phys. Lett. B **196**, 175 (1987).
- [20] M. Carrington, Phys. Rev. D **45**, 2933 (1992).
- [21] E. Weinberg and A. Wu, Phys. Rev. D **36**, 2474 (1987).
- [22] P. Ginsparg, Nucl. Phys. **B170**, 388 (1980).
- [23] For reviews, try D. J. Gross, R. D. Pisarski, and L. G. Yaffe, Rev. Mod. Phys. **53**, 43 (1981); J. I. Kapusta, *Finite-Temperature Field Theory* (Cambridge University Press, Cambridge, England, 1989).
- [24] R. Parwani, Phys. Rev. D **45**, 4695 (1992).
- [25] L. Dolan and R. Jackiw, Phys. Rev. D **9**, 1686 (1974).
- [26] P. Arnold, Phys. Rev. D **46**, 2628 (1992).
- [27] For a discussion of the gauge dependence of the effective potential at zero temperature, see N. K. Nielsen, Nucl. Phys. **B101**, 173 (1975); I. J. R. Aitchison and C. M. Fraser, Ann. Phys. (N.Y.) **146**, 1 (1984).
- [28] P. Arnold (unpublished).
- [29] M. Chanowitz, M. Furman, and I. Hinchliffe, Nucl. Phys. **B159**, 225 (1979).
- [30] J. March-Russell, Princeton University Report No. PUPT-92-1328, 1992 (unpublished).
- [31] J. Bagnasco and M. Dine, U. C. Santa Cruz SCIPP Report No. SCIPP 92/43 (unpublished).